NTNU
Innovation and Creativity

Large-scale Wind Power integration in a Hydro-Thermal Power Market

Thomas Trøtscher

Master of Science in Energy and Environment
Submission date: June 2007
Supervisor: Arne Torstein Holen, ELKRAFT
Co-supervisor: Magnus Korpås, SINTEF

Norwegian University of Science and Technology
Department of Electrical Power Engineering

Problem Description

It is expected that the share of wind power generation in the power market in the Nordic countries as well as in other parts of Europe will increase considerably in the years to come. This is expected to have an influence on power system operation as well as on the electricity prices. This thesis is focusing on the Nordpool power market area, with particular emphasis on Western Denmark where impact of wind power is very significant. The stochastic input from wind power requires the remaining generation to be operated more flexible, where also the end user flexibility becomes an interesting option. A large industrial customer that can contribute to this flexibility is particularly interesting. An example that is currently being discussed is electrolytic hydrogen production, which is a flexible load since it decouples hydrogen production and end use.

Content

The main objective of this thesis is a modeling and simulation task in order to find the influence of wind power generation on electricity prices in an open power market. The focus is on the situation in Western Denmark where the share of wind power is very significant. Important factors such as transmission capacity to neighbouring countries, influence of the Norwegian hydro system and price of thermal generation should be considered.

Also included is a case study of electrolytic hydrogen production in an area with high wind penetration, whether it is possible to make this production profitable when the production can be made flexible taking advantage of spot price variations.

Assignment given: 15. January 2007
Supervisor: Arne Torstein Holen, ELKRAFT

Preface

This report has been prepared as my Master Thesis at the Norwegian University of Science and Technology (NTNU) during the spring 2007. The work is a continuation of my Project Thesis, initiated by Elisabet Fjermestad Hagen at Norsk Hydro's New Energy section in august 2006.

Most of all, I would like to thank my co-supervisor dr.ing. Magnus Korpås at Sintef for very good support and interesting discussions during my work on the Thesis. I would also like to thank my supervisor professor Arne Torstein Holen and Elisabet Fjermestad Hagen at Norsk Hydro for valuable help during the working process.

Thomas Trötscher
June 12, 2007

Summary

This master thesis describes a quadratic programming model used to calculate the spot prices in an efficient multi-area power market. The model has been adapted to Northern Europe, with focus on Denmark West and the integration of large quantities of wind power.

In the model, demand and supply of electricity are equated, at an hourly time resolution, to find the spot price in each area. Historical load values are used to represent demand which is assumed to be completely inelastic. Supply is modeled according to the type of generation: Thermal generators are represented by piecewise linear, upward sloping, marginal cost curves. Historical wind generation data is used to model the fluctuating wind power output, and wind power is considered to have zero marginal cost. Hydro power is modeled by one aggregate reservoir for Norway and one for Sweden; the marginal cost of hydro power is set as a function of the difference between the reservoir level and the historical median reservoir level. Additionally, decentral combined heat and power plants in Denmark are considered to operate irrespective of the market.

Six separate price areas constitute the model: Denmark West, Denmark East, Norway, Sweden/Finland, Germany, and Central Europe. The areas are modeled as having no internal bottlenecks and are connected by tie-lines constrained by active power limits.

This report quantifies the impact the installed wind power capacity has on the power price in Denmark West by scaling up the wind power output in the model. Because wind power has a marginal cost close to zero, it will force prices down. The effect will be most prominent during high wind speed hours in a power system with substantial amounts of wind power. Results show that the impact is modest; average power prices fall by only 10% if the installed wind power capacity is doubled, and thermal generation will set the power price in all hours until wind energy exceeds 50% of domestic demand in Denmark.

Since prices fall the most during hours with high wind power output, income to wind turbine owners will decline quickly as the installed capacity

becomes large. The effect is most pronounced at wind energy shares above 40%, thereafter the income – per MWh sold – falls rapidly. In absence of government subventions, this effect will limit the economically viable level of installed wind power capacity.

Expansion of the cross-border transmission capacity and higher thermal generation costs can both help offset the income reduction to wind turbine owners from higher wind power penetration. Alone, a 30% increase in thermal generation costs can allow 50% of wind energy and still retain todays income to wind turbine owners. Use of the Norwegian hydro reservoirs to balance out fluctuations in wind power output is found to stabilize and reduce the price. This benefits both consumers and wind turbine owners in Denmark. Expansion of transmission capacity to Norway will further stabilize the price; a new 1000MW cable lets the Danish market easily accomodate 50% wind energy.

With lower and more volatile prices as a result of high wind power penetration, a load can profit by being flexible. Water electrolysis is one such load; it uses electricity to produce hydrogen, and production can quickly be ramped up and down in accordance with the power price. Presently, steam methane reforming is the least expensive method of producing hydrogen, but with higher wind power penetration, electrolysis might become competitive. Using a previously developed model to assess the cost of electrolysis, in combination with the power market model developed here, this report finds that wind energy must exceed 85% of domestic demand in Denmark, combined with higher natural gas prices, for electrolysis to break even with steam methane reforming.

Contents

List of Figures

List of Tables

Part I

Modeling the influence of wind power on electricity prices in Denmark-West

Chapter 1

Introduction

1.1 Motivation

Europe has ambitious goals for wind energy. The voice of the wind energy industry, the European Wind Energy Association, has set a goal for Europe to reach 75GW of installed wind power capacity by 2010 [1]. Denmark has long been at the forefront of development, in 2006 wind energy covered 17% of energy demand [2]. Together with a quickly expanding wind industry in Germany, the region is on its way to become dominated by wind power. Because of the intermittent nature of wind and the low marginal costs of wind energy this trend poses new questions regarding the effect on the power system and the power market.

This report will address one of these questions, namely how higher wind power penetration will affect the power prices in Denmark West. The motivation for this work was originally to analyze the profitability of electrolytic hydrogen production in a future power system with a high share of renewables. In preliminary work [3] it was found that an increased share of wind power might prove vital in keeping electricity prices low, and since the cost of water electrolysis is mainly determined by the electricity price, the focus moved to investigate the impact of wind power on power prices. Denmark West was selected for the study because it has the highest share of wind energy in the world.

1.2 Previous work

With the rapid growth in installed wind power world-wide, the study of large scale integration of wind power in the power system has been intensified. So far, technical topics have dominated the litterature. For the Danish power

system, several studies have investigated the effect of increased wind power penetration on the demand for ancillary services (voltage and frequency stabilization) [4], [5] and the need for regulating reserves (secondary reserves) [6], [7].

In general, it is found that in order to integrate high shares of wind power (above ≈25%), the flexibility of the power system must be improved substantially. Unlike traditional operation of the power system, where central stations alone supply ancillary services, wind power and distributed combined heat and power units will need to take part in the balancing.

The topic of this report is not concerned with the technological aspects of wind power integration. It merely assumes that solutions will be found that enable integration of any desireable amount of wind power. However, even with technical solutions in place, wind power needs to be handled at the power market. A limited amount of work has been carried out in this field. In 2004, a model to evaluate the impact of wind power was developed as part of the WILMAR (Wind Power Integration in Liberalised Electricity Markets) project [8]. It is a stochastic linear optimization model that considers both the spot market and the markets for reserves and ancillary services. The model was applied to the German market, and optimal system operation simulated under the condition of uncertain wind power output. Results focused on the price difference between the day-ahead and intra-day markets and transmission bottlenecks.

The main difference to the model developed in this report is the stochastic element and the level of detail. This report considers a much larger geographical area that is less detailed. Additionally, only the spot market is analyzed, and the focus will be on Denmark West and the impact on spot prices there.

An analysis of the short term impact of wind power on the spot price and the regulating price has been carried out for Denmark West [9]. The spot price analysis was performed by comparing the spot price in western Denmark minus the NordPool system price to domestic consumption minus wind power. A slight tendency that high wind power generation leads to lower prices was found, but no strong relationship established. The report gives no assessment of how or whether the relationship will change if the installed wind power capacity is increased. However, the relationship can hardly be expected to be linear in terms of installed wind power capacity; consequently the results can not be extended to a power system with a far higher share of wind power.

For the Nordic electricity market, simulation of large-scale wind power production has been conducted using the EMPS model in [10]. The EMPS model (see [11]) is a multi-area power market simulator for Norway, Sweden, Finland, Denmark, and Central Europe. Focus is on Norway, being modelled

as 12 areas, while Central Europe is a single area. The study used weekly time resolution to simulate system operation for shares of wind energy ranging from 4–12% of total demand in the Nordic countries. The study focused both on environmental aspects – like reduction in carbon dioxide emissions – and economic aspects, like power prices. Results from the report indicate that wind power will reduce the power price at a rate of 16 DKK/MWh per 10TWh of new wind power installed.

The most prominent differences to the model developed in this report is the time resolution used. With weekly time resolution, the fluctuating nature of wind can not be captured as well as with an hourly resolution as is used here. Also, the geographical focus of this report will be on Denmark West, where the highest share of wind energy is installed, as opposed to Norway.

1.3 Scope and outline

This report is devided into two parts. In part I a power market model of Northern Europe is developed. Emphasis is put on Denmark West and neighboring countries. The model simulates hourly (spot) power prices. By increasing the share of wind power in the power market model, statements can be made regarding the impact of wind power on prices.

The model is limited to investigate a given power system configured by the user, and does not tell whether such a system is technically or economically viable. Also, the model is restricted to spot prices; the balancing market, which probably will be strongly influenced by wind power, is not considered. The strength of the model lies in its simplicity and ability to assess the relative impact of various parameters on the price. There are better options if the goal is to predict exact spot prices.

Part II is devoted to a case study of electrolytic hydrogen production in a future Denmark. The analysis uses simulation output from part I to assess the cost reduction of electrolysis when the wind power share in the system rises. Profitability is considered qualitatively by comparing the process of water electrolysis to that of steam methane reforming.

Chapter 2

Power market model

This chapter describes a power market model for northern Europe. The purpose of this model is to assess the impact of increased wind power generation in western Denmark (Jutland/Fyn) on electricity spot prices there. In particular, it is of interest to determine what type of power plant becomes the marginal producer (i.e. the price setter) at different levels of installed wind power capacity. However, the model can easily be adapted to other purposes. Naturally, emphasis has first and foremost been placed on modeling electricity supply and demand in Denmark West. Countries connected to Denmark west by transmission lines have also been modeled to provide Denmark west with import and export capabilities in the model.

Section 2.1 gives an overview of the geographic area covered by the model and its principal workings. Section 2.2 describes how different types of generation are represented and how parameters are fitted to market data. Demand for electricity is covered by section 2.3 and transmission of power in section 2.4. Finally section 2.5 presents a summary of the model and assumptions taken.

2.1 Model overview

Figure 2.1 shows Denmark West and all price areas that are connected to it. For the purpose of this model, some areas that in reality are separate pricing areas have been aggregated. Most notably, the whole UCTE region is lumped into one large pricing area. The area specific descriptions below explain which simplifications have been done. Generally, price areas connected directly to Denmark West are modeled separately, areas 2 degrees away have been lumped together, and areas 3 or more degrees away are not modeled at all. Thus this model with the specific parameters presented here is strictly

developed to assess prices in Western Denmark. To give any reliable assertion about neighbouring countries, other pricing areas would need to be modeled. This could easily be done as adding new areas or subdividing existing ones is a simple process. However more work would need to go into data acquisition.

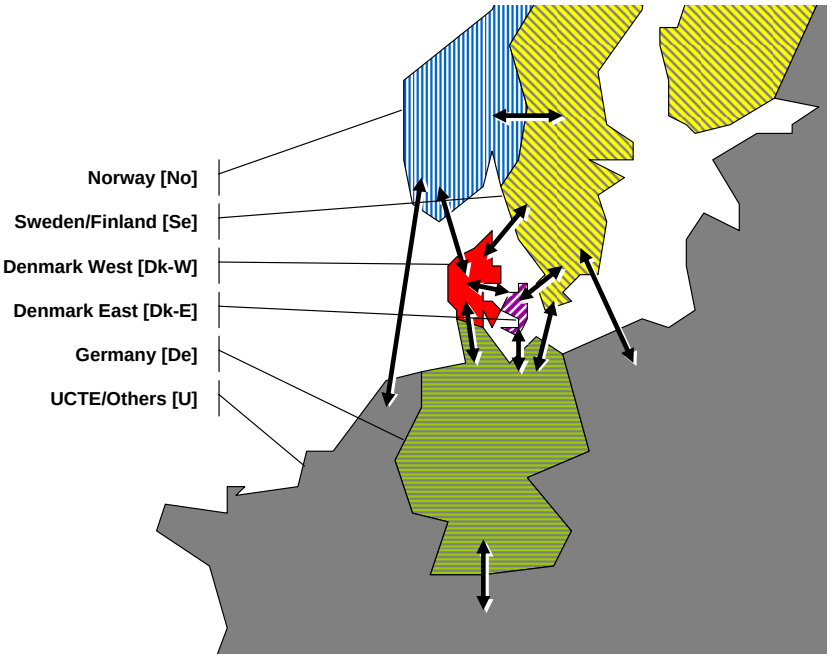

Figure 2.1: Geographic area covered by the model. Within each colored area there are assumed to be no bottlenecks. Arrows indicate constrained transmission lines between areas.

2.1.1 Area specific descriptions

The following is a short description of the characteristics of each price area as defined in figure 2.1. Two different electrical systems are part of the geographic area covered by the model. They are governed by the organization for cooperation of Nordic transmission system operators (NORDEL) and the Union for the Co-ordination of Transmission of Electricity (UCTE). Areas No, Se and Dk-E are part of the NORDEL system. Areas Dk-W, De and U are part of the UCTE system. The systems do not operate synchronously, therefore connections between these two systems are achieved by using high voltage direct current (HVDC) cables.

Denmark West (Dk-W)

Denmark West is characterised by a high share of wind power and combined heat and power (CHP) generators. It consists of a single price area at the Nord Pool power exchange. The internal grid has no noticeable bottlenecks and it is connected to Norway and Sweden by HVDC cables and to Germany by 400kV, 220kV and 150kV overhead lines.

Projected changes Denmark aims for wind energy to cover 50% of electricity supply by 2030. The main focus of this study is to assess the impact of such an increase on power prices. A HVDC cable between Dk-E and Dk-W is expected to be comissioned in 2009/2010, and this has been taken into consideration.

Denmark East (Dk-E)

Denmark East is similar to Denmark West, but with a somewhat lower share of wind power. It is also a single price area at Nord Pool.

Norway (No)

Hydro power accounts for around 99% of all electricity supply in Norway. It is split into three price areas, southern, middle and northern Norway. These three price areas have been lumped together. Trade is conducted at Nord Pool.

Projected changes A HVDC cable to Netherlands is about to be commissioned and this has been taken into account. Other grid investments or capacity investments have not been considered.

Sweden/Finland (Se)

Sweden and Finland are two different pricing areas at Nord Pool that are connected with overhead lines and HVDC cables. They have been lumped together for the purpose of this model. Sweden has approximately a 45% share of hydro power, a 45% share of nuclear power and a 10% share of thermal generation on an energy basis. Finland has about equal shares of nuclear power, conventional thermal power and renewables (bio and hydro power). Finland is connected to Russia by a back-to-back HVDC link which has been neglected in this analysis.

Projected changes Sweden is expected to install some nuclear, thermal and wind power, but this has not been taken into account.

Germany

Germany is mainly dominated by conventional thermal and nuclear power with an increasing amount of wind power in the north. Germany consists of two pricing areas, one at the European Energy Exchange (EEX) and one at Nord Pool, the so called Kontek bidding area. These two areas have been lumped together.

Projected changes Germany is investing heavily in wind power, and the installed capacity is likely to continue to grow. Growth in wind power will be assumed in the analysis.

UCTE/Others (U)

This area consists of numereous countries and power exchanges. They will only have a very indirect effect on prices in Denmark West, and are therefore considered as one large price area with no internal bottlenecks.

2.1.2 Principal workings

The object of the power market model is to investigate the influence of different factors, particularly the capacity of installed wind power, on electricity prices in Denmark West. To accomplish this, the electricity spot price will be determined for every hour of a year. This will be done repeatedly with different combinations of installed wind power capacity, hydro inflow, and load.

Three important factors that determine the price level are considered:

1. Supply. All generators are assumed to offer their generation at the marginal cost of generation.
2. Demand. The entire load is assumed perfectly inelastic.
3. Trade between areas. Cross-border power flow is constrained by upper bounds on active power.

All other possible factors like losses, internal bottlenecks, collusive pricing, market power, etc., are neglected. The following three sections will detail the models for supply (section 2.2), demand (2.3), and cross-border power flow (2.4).

The model minimizes the total cost of serving loads in all price areas by selecting the cheapest available generators and utilizing available cross border transmission capacity, i.e., an optimal merit order dispatch. This is done for every hour of the year, and the outputs are the area prices, generation by all generators, and power flow on all tie lines. In efficient markets, total system costs are minimized because of competition, and the outcome is the same as for a central optimal dispatch of generators.

Each generator is specified by a linear marginal cost curve, or in other words, a quadratic cost function. Thus a quadratic programming (QP) algorithm is employed to solve the cost minimization problem. The shadow price for the load in Denmark West is taken as the area price.

Table 2.1: Nomenclature

Symbol	*Description*
I, i, j	Set I of areas denoted by index i or j
G, g	Set G of generators g
H, h	Set H of hydro generators/reservoirs h, H is a subset of G
t	Index denoting the hour of a year
$C_g(x_g)$	Cost of generation for generator g as a function of power output [DDK/h]
$MC_g(x_g)$	Marginal cost of generation for generator g as a function of power output [DDK/MWh]
$x_g(t)$	Power generated by generator g during hour t [MWh/h]
$L_i(t)$	Power consumed by loads in area i during hour t [MWh/h]
$r_h(t)$	Level in hydro reservoir h at the beginning of hour t [MWh]
$i_h(t)$	Inflow to hydro reservoir h at time t [MWh]
$s_h(t)$	Spill from hydro reservoir h at time t [MWh]
$w_h(t)$	Water value for hydro reservoir h at time t [DKK/[MWh]
$r_{ref,h}(t)$	Median reference level for hydro reservoir h at time t [MWh]
$r_{max,h}(t)$	Upper bound on the level in hydro reservoir h [MWh]]
$P_{ref,g}$	Reference price [DKK]
$\kappa_{i,j}$	Transmission constraint on line from area i to area j [MW]
$x_{max,g}$	Upper bound on generator output [MW]
$x_{min,g}$	Lower bound on generator output [MW]
β	Coefficients of regression

Two area example

In the case of two interconnected price areas with one generator each the optimization model would look like in equation 2.1. See table 2.1 for explanation of symbols used throughout the text.

$$\begin{aligned}
\min \Big[C_1 + C_2\Big] = \min\Big[&A_1 \cdot x_1 + \frac{1}{2}B_1 \cdot x_1^2 + A_2 \cdot x_2 + \frac{1}{2}B_2 \cdot x_2^2\Big] \\
\text{s.t.} \quad & x_1 + x_2 = L_1 + L_2 \\
\text{s.t.} \quad & x_1 - L_1 \leq \kappa_{1,2} \\
\text{s.t.} \quad & x_2 - L_2 \leq \kappa_{2,1} \\
\text{s.t.} \quad & x_{min,1} \leq x_1 \leq x_{max,1} \\
\text{s.t.} \quad & x_{min,2} \leq x_2 \leq x_{max,2}
\end{aligned} \tag{2.1}$$

Solving equation 2.1 would return x_1 and x_2, i.e., the power generated by the two generators in area 1 and 2. The (shadow) price of electricity in area 1 is by definition equal to the increase in costs when increasing the load in area 1 by an arbitrarily small amount, and vice versa for area 2. If the transmission line between area 1 and 2 is not fully loaded, the price will be identical in the two areas.

QP algorithm

To solve the full QP problem, MatLab's internal QP solver `quadprog` is used. For some parameter-sets this solver fails; then the nonlinear constrained problem solver `fmincon` is used instead. The latter needs about twice the time to compute the solution.

A QP problem can be formulated on matrix form as in equations 2.2. This is also the way `quadprog` and `fmincon` takes its arguments.

$$\begin{aligned}
\min \ & \mathbf{f}'\mathbf{x} + \frac{1}{2}\mathbf{H}\mathbf{x}^2 \\
\text{s.t.} \quad & \mathbf{A}\mathbf{x} \leq \mathbf{b} \\
\text{s.t.} \quad & \mathbf{A_{eq}}\mathbf{x} = \mathbf{b_{eq}} \\
\text{s.t.} \quad & \mathbf{lb} \leq \mathbf{x} \leq \mathbf{ub}
\end{aligned} \tag{2.2}$$

Where x is a vector of decision variables. $\mathbf{f}$ and $\mathbf{H}$ define the costs associated with $\mathbf{x}$. $\mathbf{A}$ and $\mathbf{A_{eq}}$ are matrices. $\mathbf{b}$, $\mathbf{b_{eq}}$, $\mathbf{lb}$ and $\mathbf{ub}$ are vectors of the same length as $\mathbf{x}$. For the specific problem discussed in this text the first inequality constraint is not needed.

The problem with two areas and two generators in equation 2.1 can easily be transformed into the more general form in equation 2.2. Indeed the

matrices and vectors have a characteristic form regardless of the number of generators and areas. Chapter 3 explains the MatLab program that builds these matrices and solves the QP problem.

2.2 Modeling supply

Electricity is generated from many different energy sources, and each type of power plant must be operated by different rules to maximise profits to its owners. The object of this section is to devise some general and simple methods for the operation of each type of power plant. To keep the model computational effective and manageable, generators with similar characteristics in the same price area are aggregated. The interface between each generator and the overall model is a marginal cost curve as defined in equation 2.3, as well as maximum and minimum limits on generation.

$$MC_g(x_g) = A_g + B_g \cdot x_g \quad [\text{DKK/MWh}] \tag{2.3}$$

Parameters A_g and B_g must be calculated for each generator g and be passed on to the optimization algorithm for each time step. Table 2.5 toward the end of this chapter gives a summary of the marginal cost for all generators in all areas.

2.2.1 Conventional thermal power

Operation cost of conventional thermal power is largely determined by the fuel (coal, gas, oil, bio, waste) price and the power generation efficiency. Additionally, management, maintenance, and operation must be paid for in the short run. Thus, the short run marginal costs (SMC) of thermal power generation can be split into two parts, one determined by fuel costs, and one independent of fuel costs. Because this model assumes perfectly competitive markets, bidding at SMC is optimal, and fitting equation 2.3 to the marginal cost curve should provide reasonable results.

Additionally, thermal and nuclear power plants need periodic overhauls. Most of these are carried through during the summer when the load is low. To capture this effect, the available capacity of thermal power plants is reduced in accordance with the "non-available capacity due to thermal power plant overhauls in UCTE 2005" [12], see figure 2.2.

Determining the SMC of thermal power plants

Thermal power plants are used in all price areas except Norway, and the SMC will likely differ somewhat depending on the dominant fuel type and

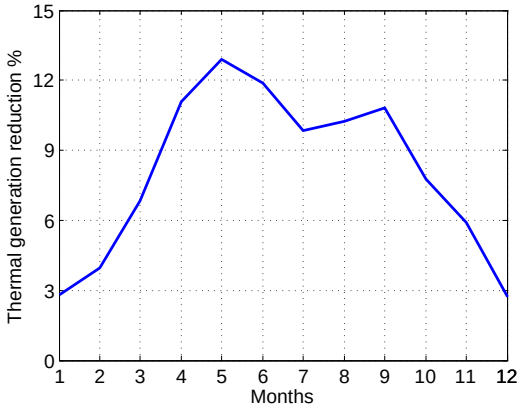

Figure 2.2: Aggregated overhaul schedule for thermal power plants.

the technology level. In the following, the aggregated SMC of thermal power plants in each price area is estimated from market data or adapted from existing work.

Denmark West The aggregated marginal cost curve of thermal power plants is estimated from spot prices and generation by central power plants. Central power stations are largely conventional thermal CHP power plants in Denmark, and aggregated generation data is easily available. It is assumed that a central power plant always is the marginal producer, and not a wind turbine or a decentral CHP plant. Further, it is presumed that the aggregated SMC curve can be approximated by a linear relationship as in equation 2.3.

During hours when all cross-border transmission capacity is on its limits, there will be a generator inside the relevant price area that is the marginal producer and thus sets the price; consequently these hours must be studied to determine the SMC curve of generators inside the area of interest. By using other hours it would not be possible to determine if the marginal producer was from another price area.

The hours of interest are extracted by comparing the hourly spot flow on the tie-lines to Germany, Norway, and Sweden to the limit for that particular hour. When all lines are constrained in either one of the two possible directions, the price in Denmark West and the generation by central stations is stored as a pair. It was iterated through all hours between 1.1.2000 and 31.12.2006. All data needed is available at the website of the Danish TSO, Energinet [2].

Figure 2.3 shows the SMC curve for Denmark West estimated from price/-generation pairs as described above. Prices have been adjusted for the oil

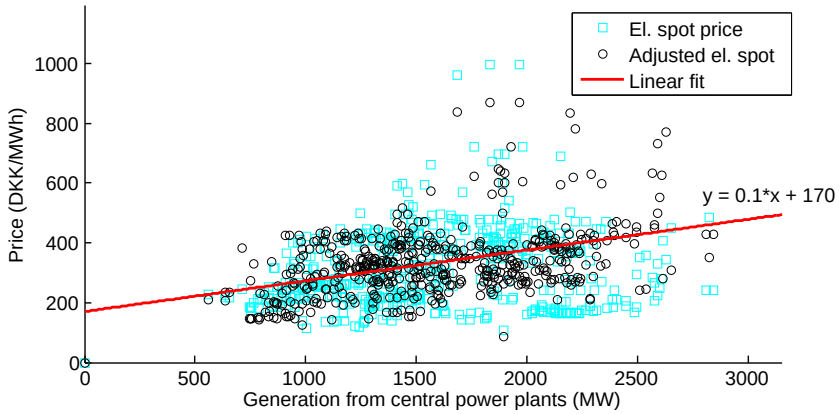

Figure 2.3: Short run marginal cost curve for Denmark West estimated from spot prices and electricity generation in hours when all cross border transmission capacity is on limits.

price (*Brent Blend*) as this is the most easily available index which is price correlated to other fossil fuels like gas and coal. A reference oil price (Brent blend) of 46$ per barrel was used, and prices where adjusted by multiplying with the reference price and divide by the concurrent oil price. This gives the same linear fit as for the unadjusted data, but a better concentration around the regression line.

Most of the central power stations in Denmark are CHP plants with relatively low costs, in addition some (270 MW) gas turbines are installed to provide peaking power. These units are modeled separately as one 135MW unit in Denmark-West and one in Denmark-East with assumed marginal cost ranging from 500DKK/MWh to 900DKK/MWh.

Denmark East The same procedure as for Denmark-West was used to determine the SMC curve of generators. The only difference between the two is that the available data period was shorter (5.10.2005 – 3.4.2007). Similar results were obtained, the main distinction being a somewhat lower slope on the fitted line. Figure 2.4 shows the linear fit.

Sweden/Finland Neither available cost curves nor the same data basis as for Denmark was available when outlining the SMC for generators in Sweden and Finland. A combination of figures for installed capacity and electricity generation from [13] and assumptions about generation costs yielded the marginal cost parameters as summarized in table 2.5.

The better part of conventional thermal generation is done by relatively low cost CHP plants. There is however installed around 5600MW of condens-

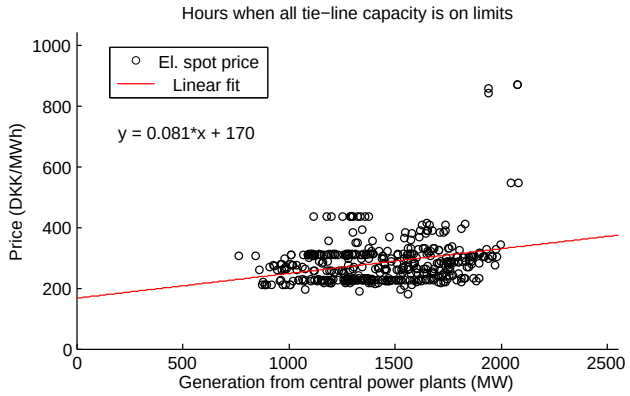

Figure 2.4: Short run marginal cost curve for Denmark East estimated from spot prices and electricity generation in hours when all cross border transmission capacity is on limits.

ing thermal power in Sweden and Finland, but on average it operates less than 1000 hours per year and can be regarded as high cost peaking power.

Germany A marginal cost curve for conventional thermal power in Germany was adapted from [14] and [12]. It should be noted that [14] estimates the installed capacity to exceed UCTE numbers by 20GW. This report uses UCTE figures for installed capacity.

Hydro power plants are assumed to operate as thermal power in Germany, and will likely run at 100% capacity utilization because of low costs. As German hydro power has a real capacity utilization of 35%, the installed power is reduced from 9.1GW to 3.19GW in the model. This, on the other hand, underrates the flexibility of hydro power, but is considered a better approximation than greatly exaggerating the yearly production. A better approximation of hydro power in Germany would be to use the single reservoir model developed for Norway and Sweden. Since the data needed was unavailable and the impact probably of little influence to the final result, this was not done.

Non fuel operation and maintenance cost are assumed as in table 2.2. The resulting supply curve is shown in figure 2.5. Generation from wind power and nuclear power comes in addition to the thermal power shown here.

UCTE/others The remaining area designated by UCTE/others is modeled based on installed capacities in the UCTE region excluding Germany. Having little direct effect on electricity prices in Denmark-West a ballpark estimate of marginal costs is considered sufficient. All generation capacity in

Table 2.2: Non fuel O&M assumptions for Germany (Own assumptions).

Type	*Cost*
Nuclear power plants	48 [DKK/MWh]
Conventional thermal power plants	40 [DKK/MWh]
Hydro power stations	24 [DKK/MWh]

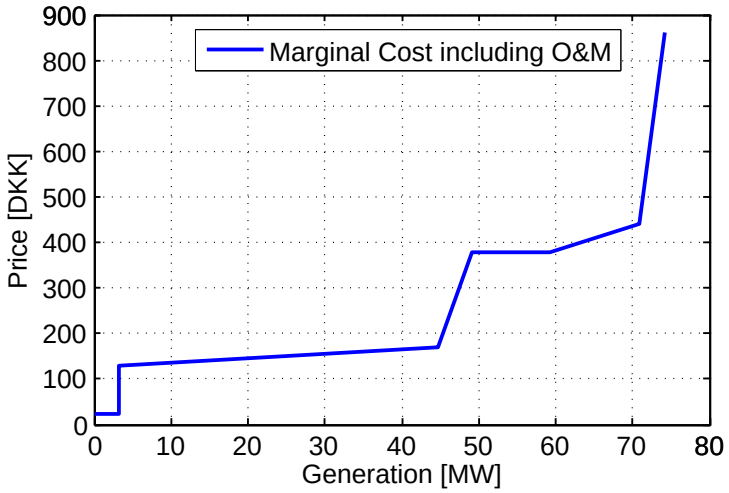

Figure 2.5: Marginal cost curve for conventional thermal power generation in Germany.

UCTE/Others is assumed to operate like conventional thermal power. Figure 2.6 shows the SMC for this area with the addition of indicators for average peak, super-peak and night time demand.

2.2.2 Hydro power

Production planning of hydro power has received much attention in Norway, and sophisticated models have been developed mainly based on load and precipitation forecasts and price expectations, see for instance [15]. As hydro power plants have virtually no operation costs, another approach than marginal cost based bidding has to be employed to optimize operation. Water in the reservoirs is per se free, but because it is a scarce resource it is valuable. The *water value* is the value of the next unit (in MWh) of water to be used in generation, and determining this value is necessary for effective production planning. When hydro reservoirs are filled to the point where they run over the water value is zero.

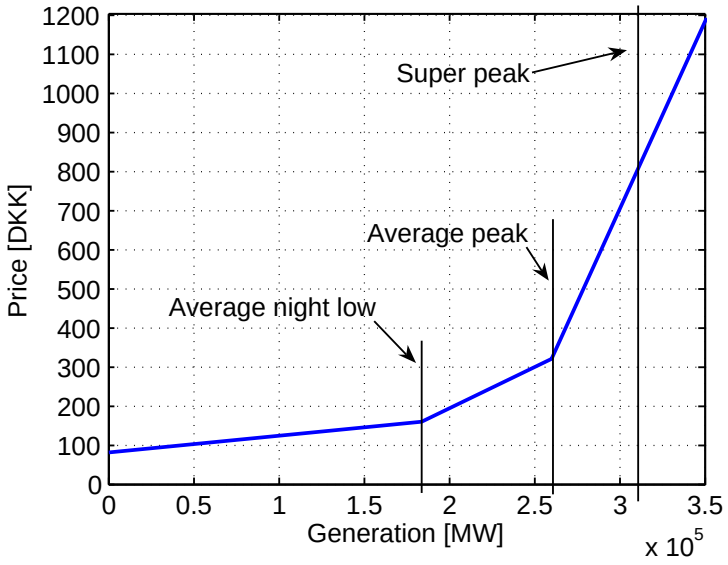

Figure 2.6: Marginal cost curve for conventional thermal power generation in UCTE excluding Germany. Indicators are for domestic demand.

Using state-of-the-art models in calculating the water value would require much computational effort and be outside the scope of this model. Therefore, a model based on the observed behavior of hydro power plants in Norway has been developed. In the following, it is assumed that the water value equals the weekly average spot price for electricity in Norway. The following price observations are made with respect to the aggregated reservoir level for Norway:

1. There is no seasonal pattern in prices. By planning well, the water in the reservoirs can be spent in such a way that the water value is even throughout the year.

2. Considerable deviations from average prices do occur when reservoir levels differ from the median reservoir level for the same week. When the reservoir level is lower than normal prices tend to be higher.

3. The average price level has risen markedly during the last 7 years.

A single reservoir model for each price area with hydro power is used, e.g., Norway is represented by one reservoir and one generator. The level in the reservoir at the beginning of hour $t + 1$ is represented by equations 2.4–2.5 which is simply the previous reservoir level plus inflow minus generation and

spill (refer to table 2.1 for notation).

$$r_h(t+1) = r_h(t) + i_h(t) - x_h(t) - s_h(t) \tag{2.4}$$
$$s_h(t) = \max\left[r_h(t) + i_h(t) - x_h(t) - r_{max,h}\ ,\ 0\right] \tag{2.5}$$

Determining the water value

To determine the water value, several regression models were developed to reflect observations 1–3 above. The models were fitted to weekly average price and reservoir data for Norway for the years 2000 to 2006, 364 weeks total. Weekly aggregated median reservoir level for Norway for the years 1990 to 2005 was used as the reference level r_{ref}. In the following, the alternate models that were tested are presented along with results from statistical tests. First the following term is defined to simplify notation:

$$\Delta = \frac{r_h(t) - r_{ref,h}(t)}{r_{max,h}}$$

Table 2.3 lists the 10 models that where tested. They are combinations of different powers of the term above along with a growth term and an adjustment term.

Table 2.3: Alternate models for water value. * = selected model.

#	*Model*
1	$\beta_1 \cdot \text{sign}(\Delta)\Delta^1 + P_{ref} \cdot (1+\beta_2)^t + \beta_3$
2	$\beta_1 \cdot \text{sign}(\Delta)\Delta^2 + P_{ref} \cdot (1+\beta_2)^t + \beta_3$
3	$\beta_1 \cdot \text{sign}(\Delta)\Delta^3 + P_{ref} \cdot (1+\beta_2)^t + \beta_3$
4	$\beta_1 \cdot \text{sign}(\Delta)\Delta^4 + P_{ref} \cdot (1+\beta_2)^t + \beta_3$
5	$\beta_1 \cdot \text{sign}(\Delta)\Delta^5 + P_{ref} \cdot (1+\beta_2)^t + \beta_3$
6	$\beta_1 \cdot \text{sign}(\Delta)\Delta^1 + \beta_2 \cdot \text{sign}(\Delta)\Delta^2 + P_{ref} \cdot (1+\beta_3)^t + \beta_4$
7*	$\beta_1 \cdot \text{sign}(\Delta)\Delta^1 + \beta_2 \cdot \text{sign}(\Delta)\Delta^3 + P_{ref} \cdot (1+\beta_3)^t + \beta_4$
8	$\beta_1 \cdot \text{sign}(\Delta)\Delta^1 + \beta_2 \cdot \text{sign}(\Delta)\Delta^4 + P_{ref} \cdot (1+\beta_3)^t + \beta_4$
9	$\beta_1 \cdot \text{sign}(\Delta)\Delta^1 + \beta_2 \cdot \text{sign}(\Delta)\Delta^5 + P_{ref} \cdot (1+\beta_3)^t + \beta_4$
10	$\beta_1 \cdot \text{sign}(\Delta)\Delta^1 + \beta_2 \cdot \text{sign}(\Delta)\Delta^2 + \beta_3 \cdot \text{sign}(\Delta)\Delta^3 + \beta_4 \cdot \text{sign}(\Delta)\Delta^4 + P_{ref} \cdot (1+\beta_3)^t + \beta_4$

Statistical indicators and manual inspection of actual prices plotted along with the model output were used to decide on a model. Out of sample (OOS) tests were performed by fitting the model to the first N weeks of data and measuring the statistical properties of the following $364 - N$ data

points. This was done with N starting at 52, and steps of 26 weeks, i.e., $N = [52,\ 78,\ 104\ \ldots\ 338]$. The average of the OOS results for all 12 instances of N are reported.

As statistical indicators, the mean squared error (MSE), measured in $\left(\frac{DKK}{MWh}\right)^2$, the coefficient of determination (R^2, dimensionless), and the Theil decomposition of the MSE are reported. The Theil inequality measure decomposes the MSE into three different components: bias ($\mathrm{U^M}$), unequal variation ($\mathrm{U^S}$), and unequal covariation ($\mathrm{U^C}$) [16, p. 875 – 876], all are dimensionless. A large bias together with a large MSE indicates the means differ significantly. Unequal variation indicates the variance is different, for instance due to different trends. Unequal covariance is attributed to unsystematic noise or phase shift.

Table 2.4 lists the results from statistical tests of the 10 models. For the within-sample data R^2 and MSE is reported. For the OOS data, the Theil measures are listed in addition to the MSE and R^2.

Table 2.4: Results from statistical tests. * = selected model

	Within sample		Out of sample				
#	R^2	*MSE*	R^2	*MSE*	U^M	U^S	U^C
1	0.6693	3841.9	0.4422	49749.2	0.4432	0.1445	0.4122
2	0.7284	3155.7	0.5295	218143.2	0.4671	0.0897	0.4432
3	0.7394	3027.6	0.5673	359950.5	0.3487	0.2229	0.4283
4	0.7249	3195.6	0.5826	450318.1	0.2882	0.3685	0.3433
5	0.6987	3500.3	0.5867	515120.0	0.2907	0.4514	0.2578
6	0.7317	3116.8	0.5297	36126.6	0.3960	0.1225	0.4813
7*	0.7418	2999.4	0.5369	36814.1	0.3097	0.2175	0.4727
8	0.7432	2983.8	0.5261	39647.3	0.2589	0.3091	0.4320
9	0.7398	3023.1	0.5096	44256.9	0.2324	0.3731	0.3944
10	0.7577	2814.7	0.4947	70944.3	0.1477	0.4845	0.3677

Most models produce a somewhat similar result. As can be seen the within-sample R^2 is good for all models, e.g., the models capture the volatility well. However some models have poor out of sample results with very large MSE. Model number 7 is selected, it has good out of sample characteristics, and according to the Theil statistic most of the error is unsystematic. All things considered, the most important characteristic of the hydro power model is to exercise a stabilizing force on the generation of hydro power by adjusting the water value. The exact value is not likely to impact greatly on prices in Denmark-West.

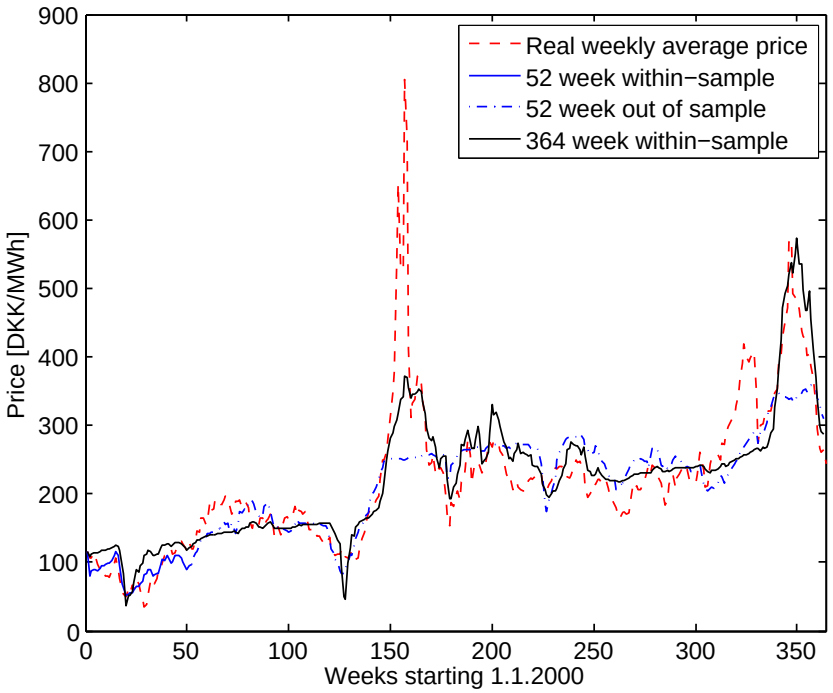

Figure 2.7: Plot of observed, fitted and predicted water value.

Figure 2.7 shows model output compared to real prices in Norway. When fitting the model using only the first 52 weeks and "predicting" the following 6 years, the two pronounced peaks are not predicted well. Using the whole data series to fit the model produces a better result. It can be seen that the model predicts the price well, and there is a logical causal relationship behind.

Simulation model

When determining the water value in the simulation, the last two terms in equation 7 from table 2.3 are replaced by the average price during 2000-2006. I.e., the parameters $\beta_3 - \beta_4$ are used only to isolate the effect of price growth. When simulating a series of 8760 hours, prices are assumed not to grow, only to fluctuate around some average level. This approach falls in line with the method used to determine the SMC of thermal generators in Denmark where prices were averaged over the same time period.

The model described above is also used for hydro power in the Sweden/Finland area. Since hydro power accounts for a far greater share of generation in NO than in SE, the same values for the parameters $\beta_1 - \beta_2$ are used for area SE as those that were fitted to NO price data.

Appendix A.4 lists the source code for the water value function and appendix A.5 lists the source code for updating the reservoir level according to equation 2.4–2.5.

Hydro inflow

The inflow $i_h(t)$ to the hydro reservoirs in NO and SE is simulation output from the "Multi-area Power-market Simulator" by SINTEF Energy Research [11] which is based on historical inflow data. 21 different series with weekly data are used for each of the two areas.

2.2.3 Wind power

Denmark and Germany have substantial shares of wind power in their power systems. Wind power typically has a low utilization time of around 1900 hours in Denmark-West, (calculated from $T_{util} = \frac{W_{el}}{P_{installed}}$, where W_{el} is the electrical energy generated by wind turbines and $P_{installed}$ is the installed power). Thus if wind power shall cover a large share of the energy used, the installed capacity must be disproportionately large. It follows that power generation from wind will be extensive during high wind speed hours, potentially covering more than demand and flooding the market.

Marginal cost of wind power

This part of the report will analyse how a large share of wind power affects power prices in Denmark-West by setting the share of energy covered by wind power generation exogenously. Since the wind is free, and unlike hydro power non-storable, a perfect market implies zero marginal cost for wind power. Some evidence from Denmark suggests that this is the case as can be seen in figure 2.8 which displays the situation in Denmark-West right after New Year 2006–2007. During some hours wind power covered the entire power demand, and prices fell to zero.

Building on this admittedly limited evidence, it is assumed that *wind power has a MC of zero*. This poses a well-founded question: What happens if the model predicts electricity prices on average far too low to cover the capital expenditure of wind turbines? In other words, a case of "a free lunch"; something inherently wrong according to economic theory. Indeed, this is a situation that must be checked for after the simulation. On the other hand, government subsidies – like a feed in price or a floor on prices – can ensure profitable conditions for wind turbine owners even with very large shares of wind power.

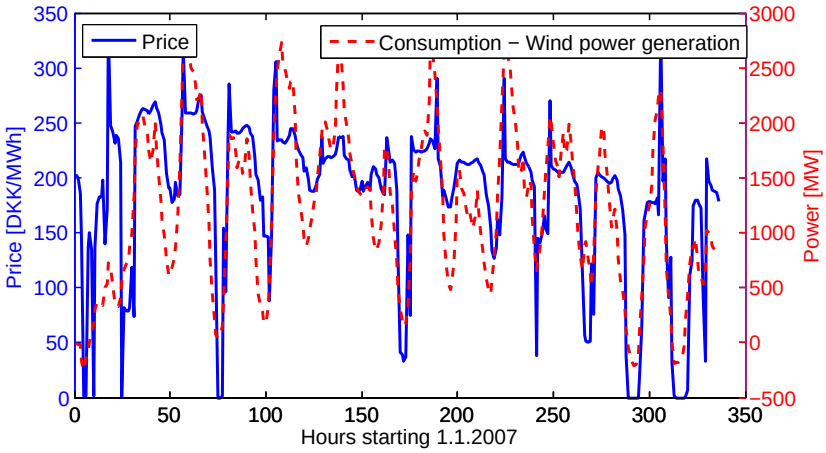

Figure 2.8: The beginning of 2007 had high wind speeds. Wind power generation covered the entire power demand during some hours, and prices fell to zero. The red dotted line shows consumption less wind power generation.

Wind generation data

Actual hourly wind generation data for the years 2000 to 2006 was used as input to the simulation for Denmark-West and Denmark-East. The data was scaled such that the installed power could be set exogenously and thereby the approximate energy output from wind power generation. Figure 2.9 shows the variability in wind power over the year for the data period. The utilization time varies between approximately 1700 and 2100 hours.

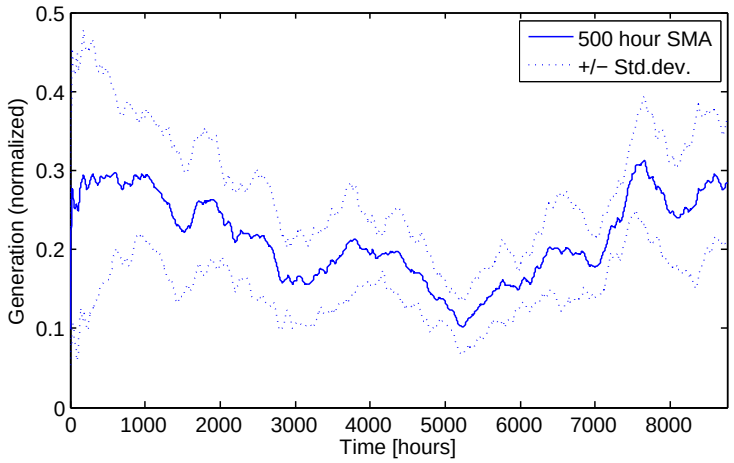

Figure 2.9: Variability in wind power generation based on time series for western Denmark years 2000–2006. The figure shows a 500 hour moving average.

Normally, higher installed wind power capacity and more wind turbines lead to less volatility in the power output because of the spatial distribution of turbines. Thus, multiplying a wind power generation series to simulate a higher share of wind power would result in too great volatility. Counter to this, data from Denmark shows increased relative volatility over the last 7 years; at the same time the total wind power capacity has risen. A possible explanation is that the rise in installed capacity is due to upgrading of the largest and best wind sites resulting in an increased spatial concentration of generation capacity. Anyhow, it is uncertain how volatility will be affected by increased capacity in Denmark; this power smoothing effect is therefore neglected. In other words, the absolute standard deviation is assumed to increase proportional to installed power.

Generation data from wind turbines in Germany have not been available to the author; thus data must be prepared from other sources. When considering wind power generation in Germany, it can neither be assumed that the wind speed there is independent of the wind speed in Denmark, nor that it is perfectly correlated. Report [17] shows how hourly variations in wind power output from turbines are correlated depending on spatial distribution. For the Nordic countries, it approximates the coefficient of correlation c_f by:

$$c_f = \mathrm{e}^{-d/500} \tag{2.6}$$

where d is the distance between two sites in kilometers. Using a distance of 300km between the main wind sites in Germany and Denmark-West gives $c_f = 0.55$.

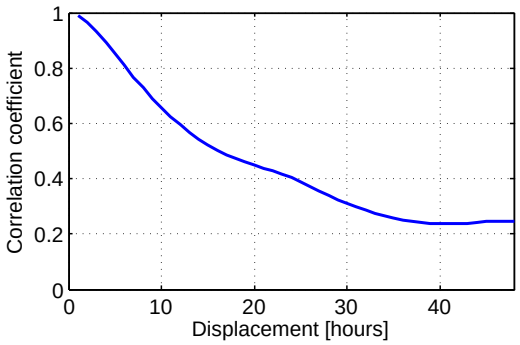

Figure 2.10: Plot of the autocorrelation of wind power generation in Denmark.

To prepare wind power data for Germany, corresponding wind data for Denmark is used, only shifted by a number of hours such that the correlation coefficient becomes 0.55. From figure 2.10 it can be seen that a displacement of 13–14 hours produces the desired effect. It is also of interest to note

that, with an average wind speed of 7 m/s, a weather front moving from Denmark would use 11.9 hours before reaching Germany. This corresponds to a correlation coefficient of 0.59 in figure 2.10, not far from the approximation given by equation 2.6. In the following a 14 hour shift will be used.

Sensitivity to temperature

Because electricity demand and generation is correlated to temperature, it is of interest to investigate whether this also is the case for wind speed. If so, wind power output cannot be assumed to be independent of demand. Based on personal experience, warm (nice) weather in the summer season usually implies little wind in Scandinavia. During the winter season the opposite is observed. To test if this is really the case for Denmark, monthly average wind power generation and temperature was separated on season and plotted in figure 2.11. To further strengthen the evidence, a similar analysis was performed on 10 coastal stations in Norway with climate data from 1966 to 2006, see appendix B.

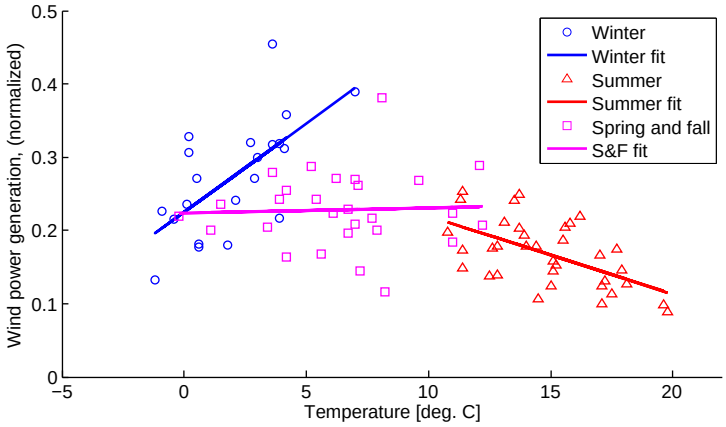

Figure 2.11: Scatter plot of wind power generation versus temperature in Denmark for the years 2000–2006 separated by season.

First of all there is a clear trend that wind speeds are higher during the winter season. Secondly, data for both Denmark and Norway indicates a relationship that falls in line with the above-mentioned experience. Cold winters see lower wind speeds as do warm summers. Therefore, it cannot be assumed that wind power generation is independent of demand. Moreover, wind power is possibly correlated to generation from combined heat and power plants (CHP) (see section 2.2.4).

2.2.4 Decentral combined heat and power

Denmark has a large share of decentral Combined Heat and Power (CHP) plants, and developing a separate model for this type of power plant is important because the power generation depends on the heat output and not necessarily on prices. CHP plants can principally be divided into two classes. Plants with a more or less fixed power:heat ratio and plants with a flexible power:heat ratio. The first type produces more power when more heat is needed, the latter can produce more heat at the cost of generating less electrical energy with the same amount of fuel. Additionally, large tanks of water are commonly used to store heat energy to generate more electricity and heat when electricity prices are high.

Sensitivity to temperature and prices

A separate model for decentral CHP will be used in Denmark West and East because they have a very high share of decentral CHP. Electricity spot price, temperature and generation data for these regions for the years 2000 to 2006 was used to explain the decentral CHP generation pattern.

Firstly, no impact of electricity spot prices on decentral CHP generation was found. In particular it was observed that the production pattern is very similar from year to year, and week to week. Let $E2000$ – $E2006$ be arrays of hourly decentral CHP generation data for the years 2000 – 2006 and let $\bar{E}$ be an array of historical means such that:

$$\bar{E}_t = \frac{1}{7}\Big(E2000_t + E2001_t + \ldots + E2006_t\Big) \quad \forall\, t \in [1 \ldots 8760]$$

Then, by subtracting $\bar{E}$ from each of the arrays $E2000$ – $E2006$ and plotting against the spot price for the corresponding years gives the scatter plot in figure 2.12. If decentral CHP generation was sensitive to prices, one would expect above average generation during high price hours and below average during low price hours. However, the figure shows no clear relationship, generation is evenly distributed around the mean. The correlation coefficient between the x-data and y-data of figure 2.12 is close to zero (0.0294) which indicates little or no effect of prices on generation.

Secondly, a simple linear regression model using monthly mean temperature (source [18] and [19]) to predict monthly average generation provides a very good statistical fit with an $R^2 = 0.952$. The observed and fitted data are shown in figure 2.13. This suggests that the operation of decentral CHP plants are governed by heat demand rather than electricity demand. Altogether, most of the variance in decentral power generation can be explained

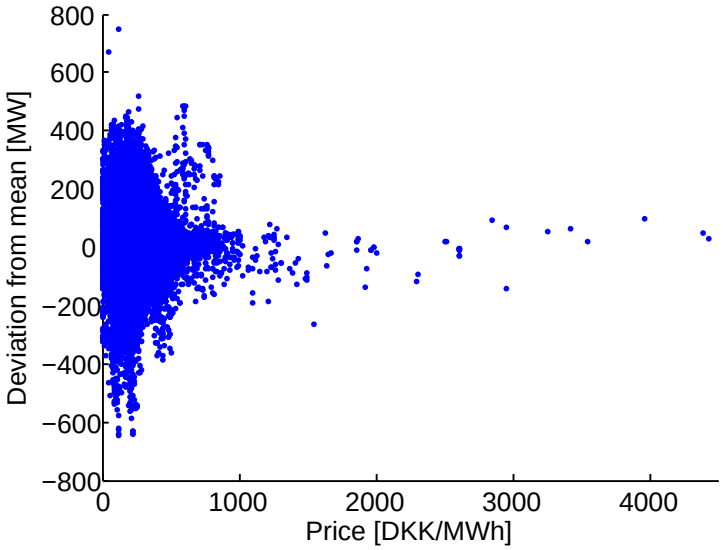

Figure 2.12: Deviation from mean decentral CHP generation versus price

by temperature and a weekly load pattern, the impact of the electricity price is neglected in this report.

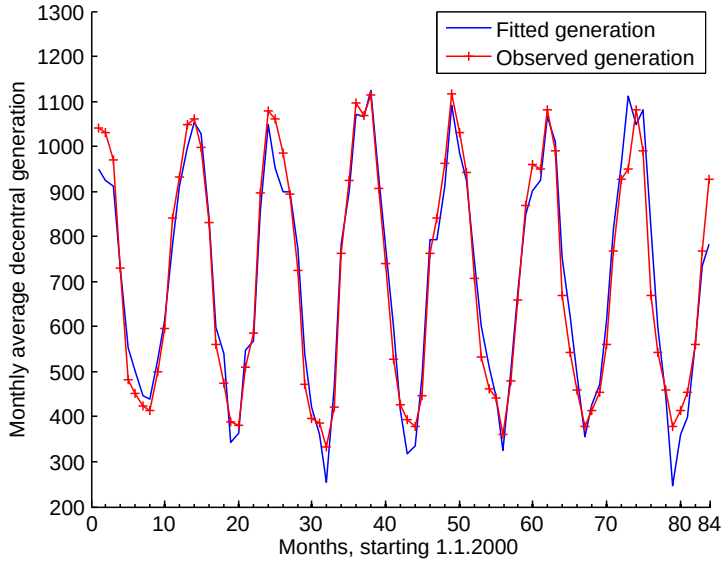

Figure 2.13: Plot of observed and fitted decentral CHP generation. The regression model is $y = \alpha + \beta \cdot T$ where T is the monthly average temperature.

As average wind speed, and thus wind power generation, proved to be significantly correlated to the mean temperature, it is of interest to investigate

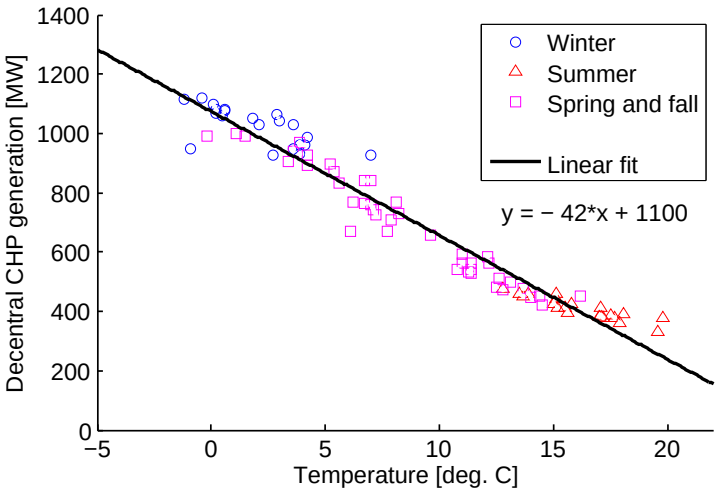

Figure 2.14: Scatter plot of decentral power generation versus temperature separated by season. Winter: December, January, February. Summer: June, July, August.

whether this is also the case for CHP generators. If so, wind power generation and decentral CHP generation cannot be assumed to be independent. Results shown in figure 2.13 suggest a clear trend on a seasonal basis, but it is also of interest to investigate whether the same is true on an inter-seasonal basis, e.g., whether a warm winter reduces electricity generation from decentral CHP generators. Indeed, this is the case as can be seen from figure 2.14 where decentral CHP generation is divided by season and plotted against temperature.

To sum up, prices seem to have no influence on decentral CHP generation as opposed to temperature and the weekly load pattern. Consequently, decentral CHP generation is taken as exogenous input in the model and any feedback from the electricity price is neglected. On the other hand, generation from wind power and CHP are correlated; thus when running a simulation, time-series from the same year must be used to capture this dependence.

2.2.5 Nuclear power

Nuclear power plants are assumed to operate like conventional thermal power plants with the exception that they have a lower bound on generation equaling 50% of available capacity. The last restriction is to ensure that nuclear power plants retain a fairly stable generation. Periodic overhauls resulting in generation capacity reduction are taken in accordance with figure 2.2.

Marginal cost for nuclear power generation is assumed to be equal across

all price areas; at 80DKK/MW it is cheaper than all other thermal generation options. The short run cost of nuclear power was adapted from [14]. The exact cost has very little effect on the price, as nuclear power is the marginal producer in very few hours.

Table 2.5: Marginal cost parameters for all generators.

Area	*g*	*Type*	A_g	B_g	$x_{min,g}$	$x_{max,g}$	*Comment*
DK-W	1	DCHP	0	0	0	1383.8	Power output set exogenously
DK-W	2	THERM.	170	0.1	0	2986.7	Mostly central CHP
DK-W	3	WIND	0	0	0	2230	Power output set exogenously
DK-W	4	PEAK	500	3	0	135	Gas turbine, very low util. time
DK-E	5	DCHP	0	0	0	819.1	Power output set exogenously
DK-E	6	THERM.	170	0.081	0	2776.3	Mostly central CHP
DK-E	7	WIND	0	0	0	772	Power output set exogenously
DK-E	8	PEAK	500	3	0	135	Gas turbine, very low util. time
NO	9	HYDRO	$w_h(t)$	0	0	23100	$w_h(t)$ Set by water value function
SE	10	HYDRO	$w_h(t)$	0	0	19167	$w_h(t)$ Set by water value function
SE	11	THERM.	160	0.0048	0	10435	Mostly CHP
SE	12	NUCL.	80	0	5816	11632	Util. time ≈ 8760
SE	13	PEAK	210	0.4191	0	5584	Condensing power, low util. time
DE	14	THERM.	24	0	0	3185	Representing hydro
DE	15	THERM.	130	9.639e-4	0	41500	Mostly coal
DE	16	THERM.	170	0.0464	0	4500	
DE	17	THERM.	378	0	0	10000	
DE	18	THERM.	378.4	0.0052	0	11750	
DE	19	PEAK	440	0.1292	0	3250	
DE	20	NUCL.	80	0	10350	20700	
DE	21	WIND	0	0	0	19000	Power output correlated to geno# 3
U	22	THERM.	80	4.348e-4	0	184000	

continued on next page...

...continued from previous page

Area	*g*	*Type*	A_g	B_g	$x_{min,g}$	$x_{max,g}$	*Comment*
U	23	THERM.	160	0.0021	0	76000	
U	24	THERM.	320	0.0096	0	70000	

2.3 Modeling demand

Electric energy is demanded by a great diversity of loads displaying a wide range of properties. It "is heavily influenced by several factors like the weather, socio-economic and demographic variables" [20]. By aggregating many loads together, it is however possible to forecast demand with great accuracy, see for instance [21]. In this model, demand for electricity is represented by a single load for each price area.

The demand for electricity is often considered to be completely inelastic in the short run, i.e., consumers do not react to price changes. This can be justified with the fact that relatively few customers are able to adjust their consumption according to price. Few studies have investigated the short term price elasticity of electricity, but [22] concludes that it generally is very low. On these grounds it is assumed that demand is perfectly inelastic, but in the following some evidence that suggest otherwise is discussed.

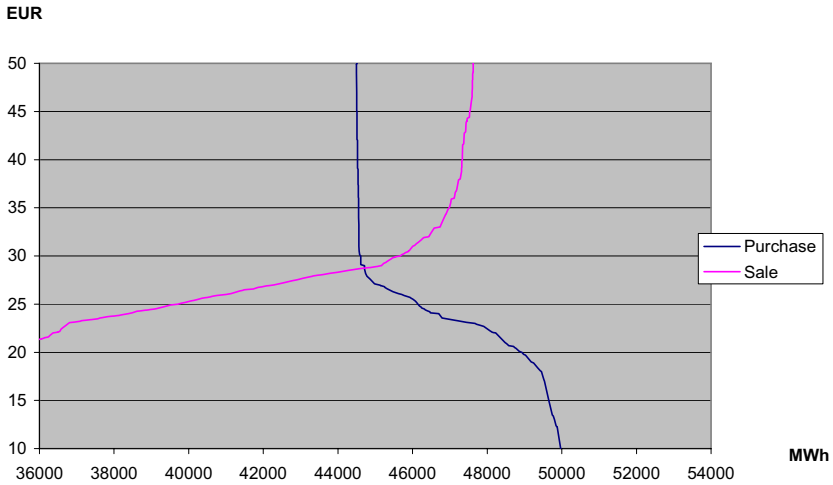

Figure 2.15: Market cross point for NordPool on 31. January 2007 10:00 – 11:00. Source: [23]

NordPool has recently started publishing bid- and ask-curves for the whole NordPool system, as does APX Power Netherlands. Figure 2.15 shows a representative market cross for the NordPool system; the characteristic

shape of the demand curve can be observed throughout the year at Nord-Pool and also in available figures at APX. The vertical part of the demand curve (purchase) is where demand is inelastic, i.e., about 44250 MWh of demand is independent of price.

The implication of assuming perfectly inelastic demand is that a generation change will affect prices more within a limited range than the case is for a demand curve as in figure 2.15. The elastic part is however small relative to the total load.

The long term responsiveness to a change in electricity prices might be significant as compared to the short run response. A study [24] does however find that the long and short run elasticities for electricity used in appliances do not differ significantly and are rather low. On the other hand, electricity used for space heating is likely to be more responsive to a price change, as several substitutes like wood and heating oil exist.

2.3.1 Load data

Actual time series of load data are used in the simulation for Norway, Sweden/Finland, Denmark-West, and Denmark-East, see table 2.6. Since demand, as seen above, is relatively own-price inelastic it should be a good estimate for a wide range of prices.

For the areas Germany and UCTE/Others, such data is not publicly available. Therefore, load data is created synthetically based on the load profile for the 3rd Wednesday each month in 2005, available in [25]. In short, the the daily profile is created by interpolating between the two nearest available load profiles, e.g., the load profile for 1. January is created by interpolating between the 3rd Wednesday in December and the 3rd Wednesday in January. Additionally, reduced demand during weekends is taken into account and normally distributed daily variations can be added to introduce some randomness. Appendix A.7 shows the full source code in MatLab format. The weekend load pattern i calculated from the weekday load patter as follows:

$$wel_t = (wdl_t - \min(wdl_t)) \cdot wb \cdot wbpeak + \min(wdl_t) \cdot wb$$

Where $\min(wdl_t)$ is the lowest load during the weekdays of the year and wel_t is the weekend load for hour t. Parameters `wb=0.9; wbpeak=0.8; stddev=0.01;` are used, corresponding to reduced weekend base load by 10%, reduced weekend peak load by 28%, and daily variations with a standard deviation of 1% of the mean load. Public holidays are not taken into account.

Table 2.6: Overview of timeseries

Area	*Type*	*Source/Comment*
DK-W	Load	energinet.dk
DK-E	Load	energinet.dk
NO	Load	NordPool ftp server
SE	Load	NordPool ftp server
DE	Load	Based on UCTE data (See section 2.3.1)
U	Load	Based on UCTE data (See section 2.3.1)
DK-W	DCHP generation	energinet.dk
DK-E	DCHP generation	energinet.dk
DK-W	Wind generation	energinet.dk/Scaled up
DK-E	Wind generation	energinet.dk
DE	Wind generation	Time-shift (See section 2.2.3)
NO	Hydro inflow	Simulated data from EMPS [11]
SE	Hydro inflow	Simulated data from EMPS [11]
All	Overhaul schedule	UCTE data from 2005 [12]
NO	Median reservoir level	NVE homepage [26]
SE	Median reservoir level	Adapted from [27]

2.4 Cross-border power flow

Constraints on power flow between areas are modelled by upper bounds on active power flow. The limits may differ in opposing directions. Transmission limits for the Nordel areas are taken from [13] and corresponding numbers for UCTE are taken from [28]. Grid reinforcements that will be completed within the next years are included. The relevant limits are summarized in table 2.7.

Table 2.7: Overview of timeseries

To, j / **From,** i	DK-W	DK-E	NO	SE	DE	U
DK-W	–	600	1000	630	1350	0
DK-E	600	–	0	1810	600	0
NO	1000	0	–	3620	0	700
SE	670	1410	3340	–	600	600
DE	950	600	0	600	–	14650
U	0	0	700	600	14650	–

2.5 Model boundaries

This section will focus on summarizing the model boundaries and assumptions with help of the causal loop diagram in figure 2.16. A causal loop diagram is used to show interdependencies of variables. See [16] for an introduction to causal loop diagrams and system dynamics. There exists two types of relations: Positive and negative, denoted by arrows with a plus (+) or minus (-) sign. If a relation is positive, and assuming that other variables are held constant, an increase in the variable the arrow is pointing from increases the variable it is pointing to and vice versa. Thus, referring to figure 2.16, one can see that if supply increases, and demand is held constant, then the price decreases.

The causal loop diagram shows the situation as seen from Denmark-West with all the other areas being denoted as "abroad". At the beginning of this chapter three factors were listed that affect the price: Supply, demand, and imports/exports. This is the heart of the diagram; supply and demand equate and form the electricity price for every hour of the year. This "equation" is the one solved by the quadratic program solver.

Section 2.2 treated supply. In each area, the marginal cost of all generators were defined. By aggregating these marginal cost curves, an upward sloping supply schedule can be derived. Thus, when prices increase, the profits of power plant owners increase and they are prepared to offer more power for sale. This constitutes a balancing loop in the diagram. In reality the price also affects the decision to build new power plants (or to mothball existing ones). These decisions are frequently associated with long time delays (denoted by a double line crossing the arrow) and are influenced by other important factors like security of supply, uncertainty in fuel prices, and environmental concerns. Altogether, these feedbacks are cut; the non-wind power capacity is constant and the installed wind capacity is varied exogenously. The possible implication is that unrealistic wind power levels can be attained.

Demand for electricity was set to be completely inelastic justified mainly by the fact that there are no good substitutes for electricity. Thus, if prices fall or rise the consumed amount stays the same. In the causal loop diagram, this corresponds to cutting the loop from price to demand.

Transmission from one area to another also helps stabilize the price. If the price abroad is higher than the price in Denmark West, export is positive (i.e. the power flow is out of the country) and vice versa. If prices between two areas differ in the long run, there is a pressure to expand the transmission capacity. However, this is a lengthy process, maybe more so than investment in new power plants, that is subject to public inquiries and international

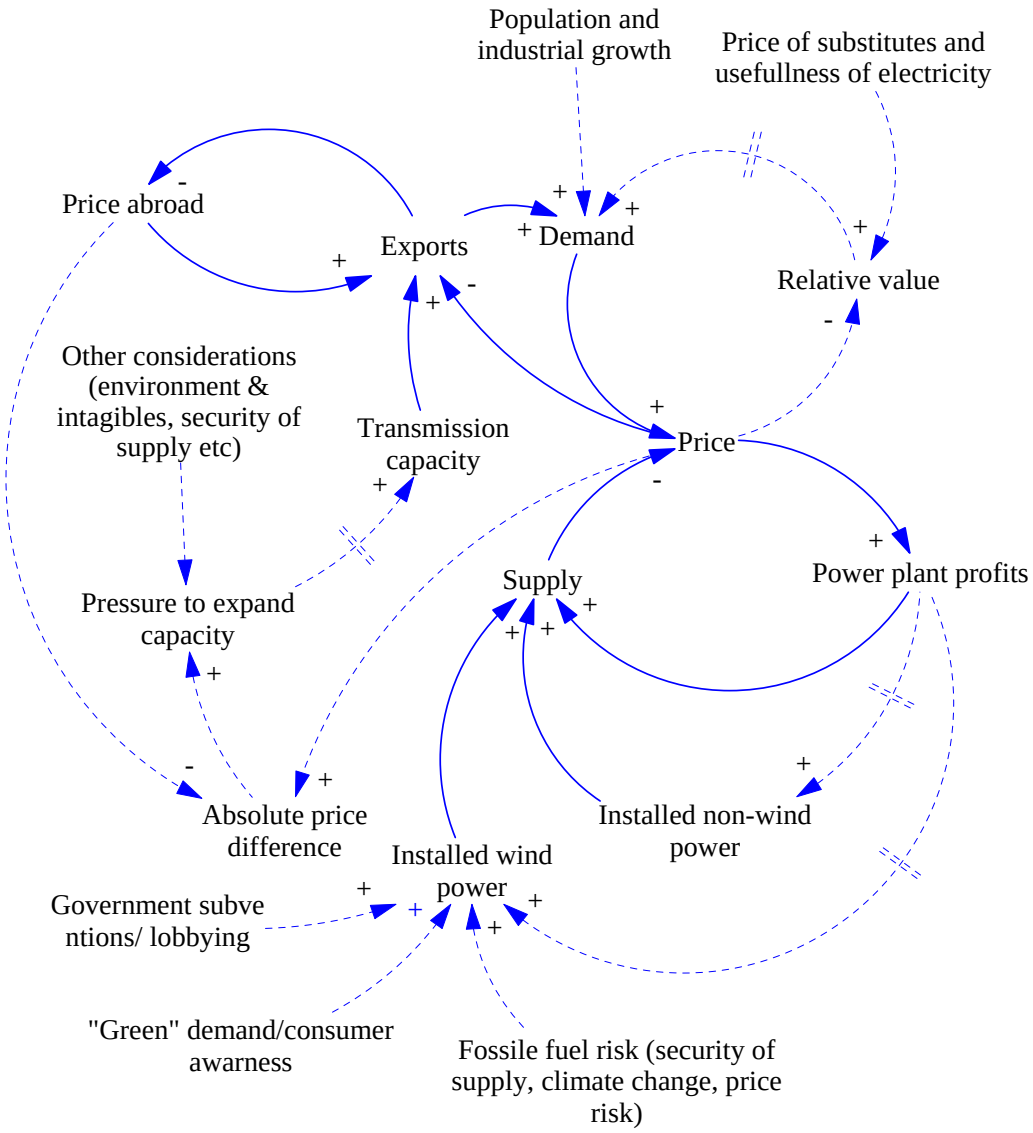

Figure 2.16: Causal loop diagram of the factors affecting the electricity price. Dashed feedbacks are ignored, only the solid-drawn relations are considered endogenous in the model.

agreements. Therefore the cross-border transmission capacity is regarded as constant, and only expansions where decisions have been taken are allowed for.

Altogether, the model developed so far tries to give an assertion about the power price in Denmark for a given power system scenario. It does not state how likely this scenario is, and it is possible to create both realistic and unrealistic scenarios. The worst pitfalls can be avoided by keeping the effect of the removed feedbacks in mind when setting the exogenous parameters.

Chapter 3

Simulation structure

This chapter explains how simulations are run using the power market model developed in chapter 2. Emphasis will be put on understanding how the theoretical model was implemented in code. The purpose is to make the model more transparent and to accommodate reproduction of results.

3.1 Program flow

By means of the flow chart in figure 3.1, the program flow will be explained. The program is started by running the Matlab script `power_market_model.m` which is listed in appendix A along with all other source code needed to run the simulation. It basically consists of two nested for-loops. In the following, a *simulation* will be referred to as running the entire script once and one *run* (of a simulation) refers to running the outer for-loop once i.e. one year. The inner for-loop cycles through all *hours* of each run.

Starting the program loads variables that are constant over all runs, sets the run counter to 1, and initializes the levels in the hydro reservoirs of Norway and Sweden at the median level. Additionally the number of runs and the combinations of exogenous time-series and installed wind power capacity for each run can be specified. I.e., it can be specified which load series, wind data series, decentral CHP generation series, hydro inflow, and installed wind power capacities to be combined for each run. By holding all exogenous parameters except one constant, it is possible to analyse the price sensitivity to that particular parameter, e.g,. using load, decentral CHP, and wind data from 2006 and variable hydro inflow would produce the sensitivity of prices in Denmark West to hydro inflow in Norway and Sweden for 2006. It is also possible to do a monte-carlo simulation by drawing random combinations of time-series to get a distribution of prices. In section 2.2.4 it was found that

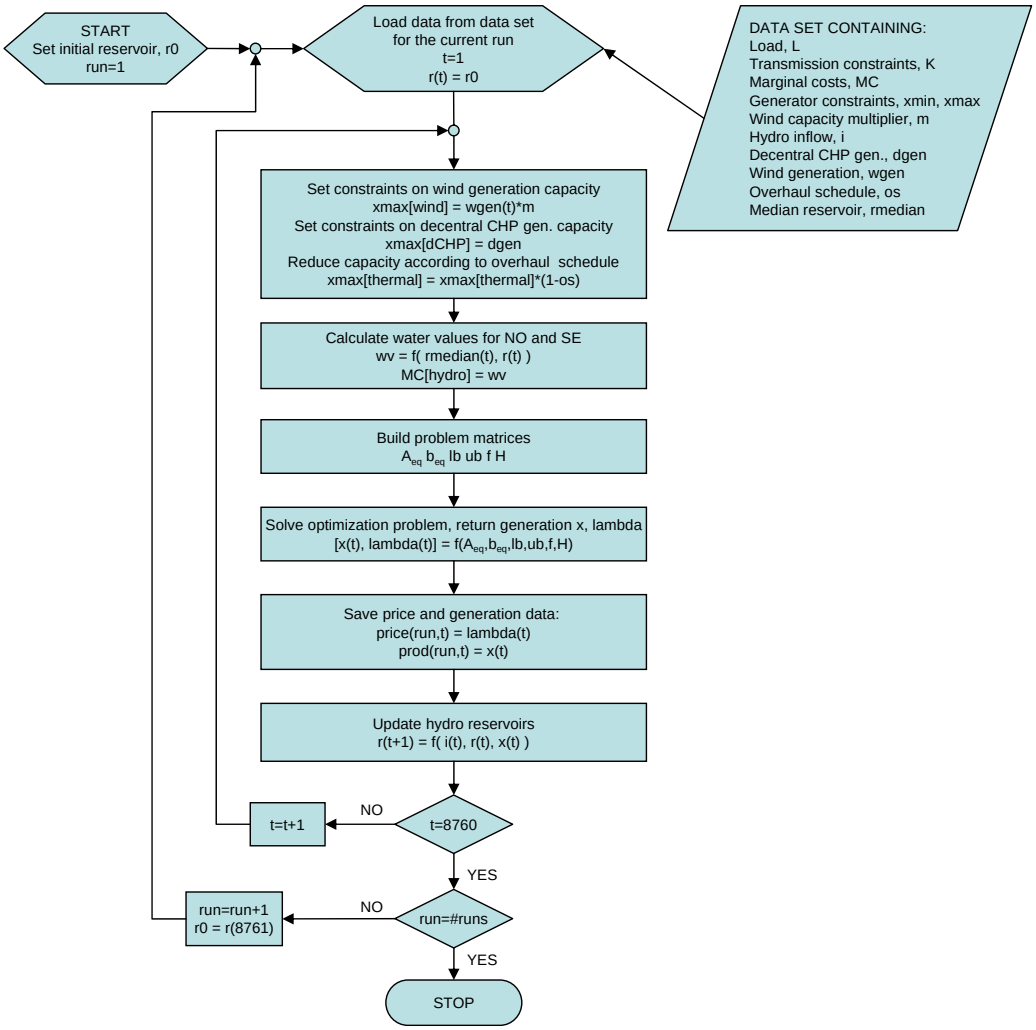

Figure 3.1: Flow chart for the simulation model.

the generation from wind power and decentral CHP are correlated through temperature. Since the load also depends on temperature, all these three factors are linked; consequently, corresponding time-series for load, wind, and decentral CHP should be used in the same run.

The next step loads all data for the current run as specified above and initializes the hour counter t. For each hour, a number of steps are performed to prepare the problem matrices. First, the maximum limit on wind generation is set to the available wind generation capacity. Since the cost of wind power is set to 0, the maximum limit will always be utilized as long as the power balance is maintained. The same procedure is repeated for decentral

CHP generation followed by reducing the maximum generation capacity of all thermal generators according to the overhaul schedule.

Based on the reservoir level in Norway and Sweden the water values for these two areas are calculated by the function in `water_value.m`. The marginal cost of the hydro generators are then set equal to the respective water value. The next step passes load, L_i, maximum and minimum generation capacities, $x_{max,g}$ and $x_{min,g}$, and marginal cost, $MC_g(x_g)$, to `merit_order.m`. This function builds the problem matrices and tries to solve the problem with the QP solver `quadprog`. If this fails, it attempts to solve the problem with a general constrained optimizer called `fmincon` which is somewhat slower.

The solver returns shadow prices (lambdas) for all constraints and power output of all generators, $x_g(t)$. The shadow price of the load in Denmark West is taken as the area price and saved together with the power output. Finally, using the function in `single_reservoir.m`, the hydro reservoir levels for the beginning of the next hour are found by adding inflow, subtracting generation, and checking for water spill. If a whole year has passed ($t = 8760$), a new run is started, and the initial hydro reservoir levels are set to the final reservoir levels of the previous run.

3.2 Problem matrices

This section describes the structure of the problem matrices as defined by equation 2.2. In contradiction to some other QP solvers, MatLab does not form the problem matrices automatically based on a set of equations. On the other hand, predefining the matrices speeds up computation time.

Let n denote the cardinality of I (the number of areas) and m the cardinality of G (the number of generators). The number of possible interconnections p is then $p = \frac{n^2-n}{2}$. By using the cost parameters A_g and B_g according to equation 2.3 it is now possible to define $\mathbf{x}$, $\mathbf{f}$ and $\mathbf{H}$ as in equations 3.1–3.3. Note that braces state matrix dimensions.

$$\mathbf{x} = \overbrace{\begin{pmatrix} x_1 & x_2 & \dots & x_m & x_{1,1} & x_{1,2} & \dots & x_{1,n} & x_{2,3} & \dots & x_{n-1,n} \end{pmatrix}^T}^{m+p} \tag{3.1}$$

$$\mathbf{f} = \overbrace{\begin{pmatrix} A_1 & A_2 & \dots & A_m & 0 & \dots & 0 \end{pmatrix}^T}^{m+p} \tag{3.2}$$

$$\mathbf{H} = \overbrace{\begin{pmatrix} B_1 & 0 & \dots & & 0 \\ 0 & B_2 & & & \\ \vdots & & \ddots & & \\ & & & B_m & \\ & & & & 0 \\ & & & & & \ddots \\ 0 & & & & & & 0 \end{pmatrix}}^{m+p} \tag{3.3}$$

Let m_i be the number of generators in area i such that $\sum_i^n m_i = m$. Then matrix $\mathbf{C_i}$ and $\mathbf{D_i}$ that constitute $\mathbf{A_{eq}}$ can be defined as in equation 3.4–3.5.

$$\mathbf{C_i} = \overbrace{\begin{pmatrix} 0 & \dots & 0 \\ \vdots & & \vdots \\ 0 & \dots & 0 \\ 1 & \dots & 1 \\ 0 & \dots & 0 \\ \vdots & & \vdots \\ 0 & \dots & 0 \end{pmatrix}}^{m_i} \begin{matrix} \left.\vphantom{\begin{matrix}a\\a\\a\end{matrix}}\right\} i-1 \\ \\ \left.\vphantom{\begin{matrix}a\\a\\a\end{matrix}}\right\} n-i \end{matrix} \tag{3.4}$$

$$\mathbf{D_i} = \overbrace{\begin{pmatrix} 0 & 0 & \dots & 0 \\ \vdots & \vdots & & \vdots \\ 0 & 0 & \dots & 0 \\ -1 & -1 & \dots & -1 \\ 1 & 0 & \dots & 0 \\ 0 & 1 & \dots & 0 \\ \vdots & \vdots & \ddots & \vdots \\ 0 & 0 & \dots & 1 \end{pmatrix}}^{n-i} \begin{matrix} \left.\vphantom{\begin{matrix}a\\a\\a\end{matrix}}\right\} i-1 \\ \\ \left.\vphantom{\begin{matrix}a\\a\\a\end{matrix}}\right\} n-i \end{matrix} \tag{3.5}$$

Matrix $\mathbf{A_{eq}}$ is constructed from several instances of $\mathbf{C_i}$ and $\mathbf{D_i}$:

$$\mathbf{A_{eq}} = \overbrace{\left(\begin{array}{ccc|ccc} \mathbf{C_1} & \dots & \mathbf{C_n} & \mathbf{D_1} & \dots & \mathbf{D_{n-1}} \end{array}\right)}^{m+p} \tag{3.6}$$

Vector $\mathbf{b_{eq}}$ is a row vector containing the load for each area.

$$\mathbf{b_{eq}} = \begin{pmatrix} L_1 & L_2 & \dots & L_n \end{pmatrix}^T \tag{3.7}$$

Once again referring to equation 2.2, the rows of the constraint $\mathbf{A_{eq}x} = \mathbf{b_{eq}}$ represent the power balance for each area. Additionally, there are upper and lower bounds on $\mathbf{x}$ representing limits on generation and power flow.

Normally, the number of interconnections is less than p and some of the variables can be removed. This greatly improves running time.

3.3 Performance, software and hardware

The model was run on a personal computer with an Intel Pentium M 1.73GHz processor, 1 GB of RAM, Windows XP, and Matlab 7.1. Approximate running time for a single run of 8760 hours with that configuration was 11 minutes. More than 98% of the running time was spent on the optimization algorithm which is a built-in function in Matlab 7.1.

Chapter 4

Results

This chapter presents results obtained with the model. Section 4.1 deals with verification of the model. Key properties are examined, output compared to real observations, and extreme value tests conducted. Section 4.2 covers the impact assessment of high wind power penetration on spot prices.

4.1 Model verification

4.1.1 Extreme value tests

These tests are designed to verify that the model responds plausibly when inputs are on their extreme values. Even though such extreme values are unlikely, it is important that no odd results like negative prices or negative reservoir levels arise.

Wind power

Figure 4.1 shows a duration diagram of the power price in Denmark-West for three cases: Present day installed wind power capacity, infinite capacity, and no capacity. With no installed wind power the prices are generally somewhat higher, but there are no problems in covering the load. With unlimited installed wind power capacity the price is zero almost all the time apart from some completely calm hours with no wind power generation.

In a Danish study from 2006 [29], the impact of wind power on power prices was investigated by asking the hypothetical question: "What would the power price have been if there had been no wind?" The report finds that consumers in western Denmark saved between 12% and 14% on the power bill during 2005. Comparable results can be obtained using the model developed in this report. By doing an extreme value test for 2005 similar to

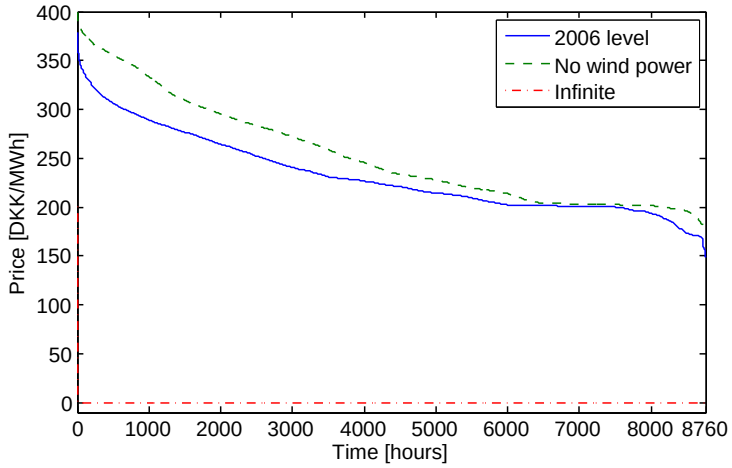

Figure 4.1: Duration curve of power prices for extreme values of installed wind power capacity compared to the (simulated) 2006 level

the one above, and multiplying the price by the load, it is possible to get total consumer expenditure on electricity with and without wind power. A comparison of the no-wind case and the 2005 case is shown in figure 4.2. Total savings amount to 12.46% of consumer expenditure placing it well within the range found in [29].

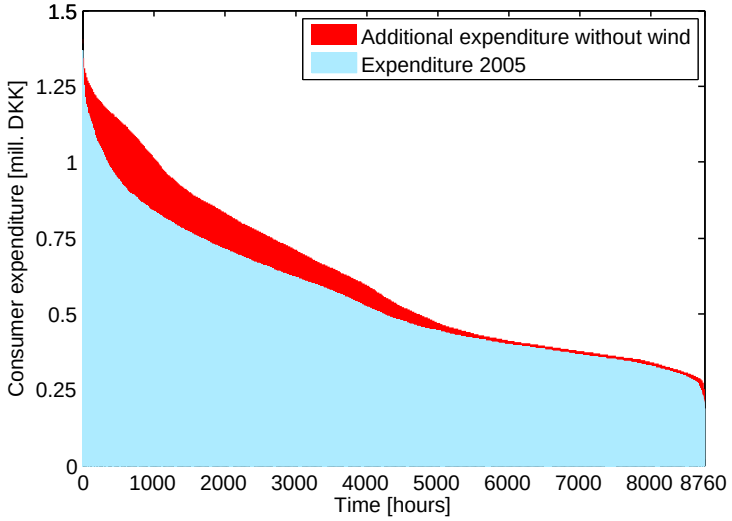

Figure 4.2: Consumer savings due to wind power equals the additional expenditure had there been no wind power in the system.

Hydro inflow

With no hydro inflow to the reservoirs in Norway and Sweden, the reservoirs are gradually emptied until the power balance collapses in Norway because the import capacity is insufficient to cover demand. At that time the algorithm exits with an error message, and the price in Norway peaks at around 3800 DKK/MWh. The reservoir level in Sweden is emptied until the water value becomes as high as the most expensive alternative generation option (around 1800 DKK/MWh). See figure 4.3.

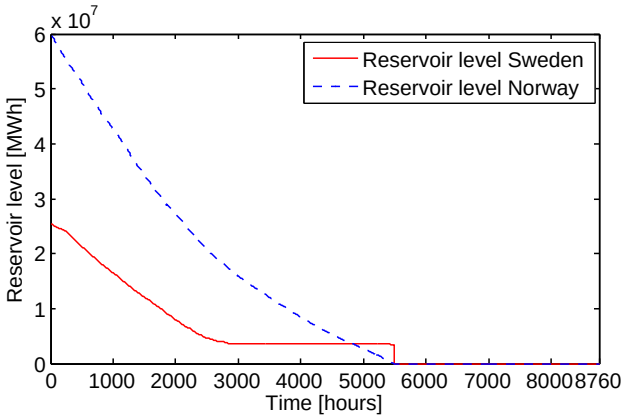

Figure 4.3: Zero inflow to the hydro reservoirs in Norway and Sweden leads to a collapse in the power balance in Norway after around 5500 hours.

Infinite hydro inflow results in the opposite situation. Reservoirs are instantly filled and the water value immediately falls to zero. All available transmission capacity is utilized to export power.

Transfer constraints

By increasing the transfer capacity such that no lines are constrained, the price becomes equal across all areas. Since the UCTE/Others region is superior in size the price effectively equals that of this area. See figure 4.4.

When the transmission capacity is reduced to zero, all areas operate as islands. For the case of Denmark-West the price generally rises as more expensive thermal power plants must be used more often. Additionally, the price falls to zero during some hours when there is excess wind power that cannot be exported. Both observations are as expected.

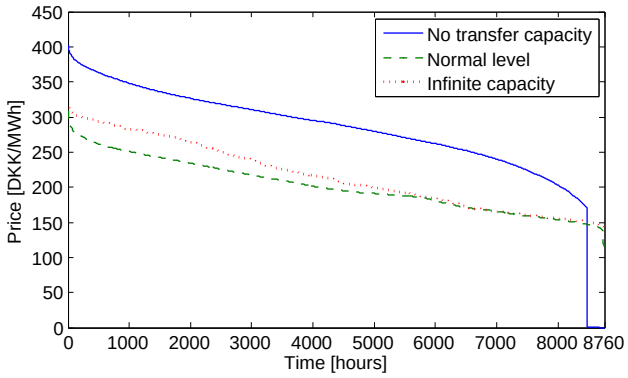

Figure 4.4: Extreme values for cross-border transmission capacity compared to the normal values of table 2.7

4.1.2 Comparison to real prices

In creating the model, most marginal cost parameters were fitted to observed market data. In doing this it was often averaged over several years, for instance in setting the average water value and fitting the marginal cost of thermal power in Denmark. Thus, simulated prices can be expected to approach the mean for the data period (2000-2006). Because prices grew during the whole period, comparing simulation results to prices from 2006 will result in too low estimates, and comparing to prices from 2000 will result in too high price estimates. Another factor that obscures the comparison is that simulated hydro inflow data from a time period earlier than 2000–2006 was used instead of the real inflow.

For the reasons listed above, the strength of this model is not to predict exact spot prices, but to analyze the relative impact of different factors. Figure 4.5 shows a duration diagram of real prices compared to simulation output. The simulation for this comparison consisted of seven runs where hydro inflow always followed the median inflow, and load, wind, and decentral CHP data for the years 2000–2006 were used. It can be seen that the simulated data has less volatility than the real data.

The same pattern can be observed by comparing the moving average of actual and simulated prices as it is done in figure 4.6. The simulation consisted of 10 runs with load, wind and decentral CHP data from 2003 and 10 randomly drawn hydro inflow series. Correlation coefficient between the mean of the 10 simulated series and the historical observed series is 0.44.

Again, the simulated data is less volatile than the real prices. The main reasons are probably: (1) That the simulation model assumes perfect competition, (2) there are no unexpected or sudden faults and outages, (3) thermal

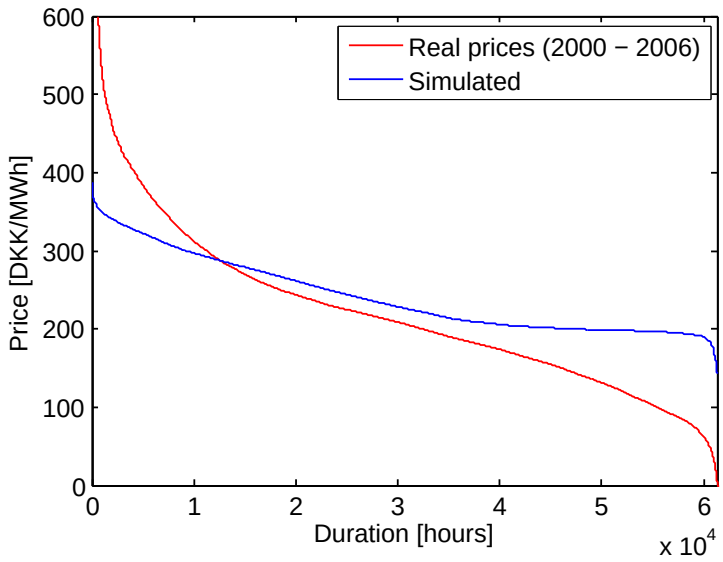

Figure 4.5: Duration diagram of simulated prices compared to the real duration diagram. The price for all 7 years have been sorted, totaling 61368 hours.

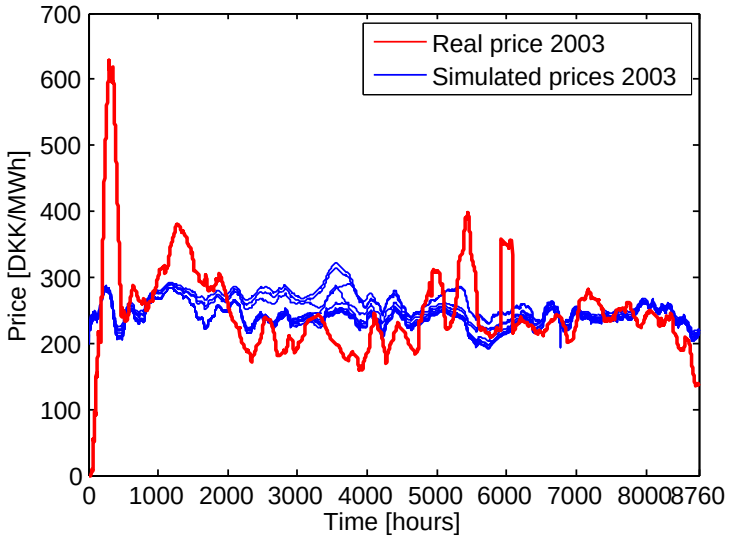

Figure 4.6: The 168-hour simple moving average of real prices and simulated prices for 2003.

generation can be ramped up and down arbitrarily (4) all transmission capacity can be used for spot trade and is always available, and (5) political signals, fear for a dry year, and the "psychology of the game" do not come into play. All these factors exercise a stabilizing force on the power price resulting in less volatility in the simulated system.

4.1.3 Power flow on tie-lines

Some random samples where tested to verify that power flows from the low to the high price area, and that there is no price difference if the transmission line is not fully loaded. Two examples of power flow on tie-lines connecting Denmark-West to Norway and Germany are shown in figure 4.7 and 4.8 along with the price difference. The transmission limit is 1000MW in both directions on the line to Norway and 1350/950MW to/from Germany. As the reader may verify, the above assertion regarding power flow holds.

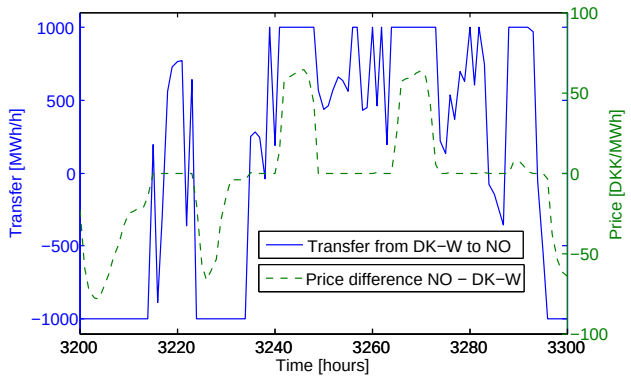

Figure 4.7: The left y-axis is the power flow from Denmark to Norway and the right y-axis is the power price in Norway minus the power price in Denmark-West. Power flows from the low price to the high price area.

4.1.4 Hydro reservoir levels

The intention of this section is to investigate how the reservoir levels and the water value vary during normal conditions. The price in Norway is plotted along with the reservoir level in figure 4.9. Because Norway is modeled as a single hydro reservoir, the price in effect equals the water value.

There is a tendency in the plotted data to exploit the reservoir capacity more compared to the real historical median level. In other words, more water is spent during the winter and less during the summer. Yet other runs

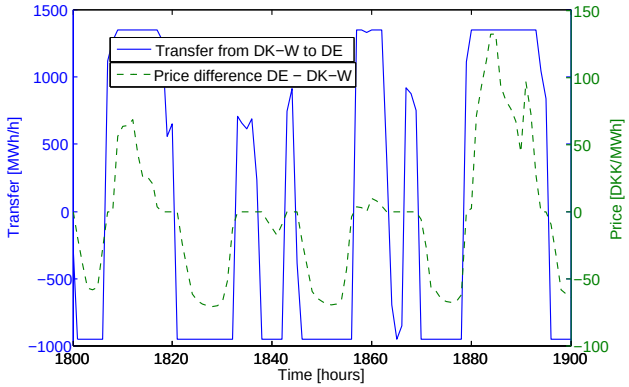

Figure 4.8: The left y-axis is the power flow from Denmark to Germany and the right y-axis is the power price in Germany minus the power price in Denmark-West. Power flows from the low price to the high price area.

with different inflow series confirm this trend, although there is considerable variation.

In contrast to the other areas, there are no diurnal variations in the power price in Norway; the reason being that the hydro power model sets a fixed water value with no slope. Deciding to build the model that way can be justified by the fact that there is no real reason that the water value should follow a diurnal pattern when the reservoir level does not.

4.2 Increased wind power penetration

In response to the worlds demand for "greener" energy, both Germany and Denmark have set goals to increase their shares of wind power. Denmark, in particular, aims for wind power to cover 50% of its energy demand by 2030 [30]. This section will use the model developed so far to assess the impact of increased wind power penetration in Germany and Denmark on power prices in Denmark West. Some of the analyzed scenarios far exceed even the most abitious goals in terms of installed wind power capacity and may be deemed unrealistic. However they are interesting from an academic viewpoint.

Installing such high shares of wind power in a power system as is discussed here is not only an economic issue, but also a technological challenge. It is implicitly taken for granted that the power system remains stable and that thermal power plants and hydro reservoirs are able to counter the fluctuating output of wind power. Current research indicates that it is possible to accommodate shares exceeding 50% even without relying on neighbouring countries to supply ancillary services [4]. Additionally, utilising the Norwe-

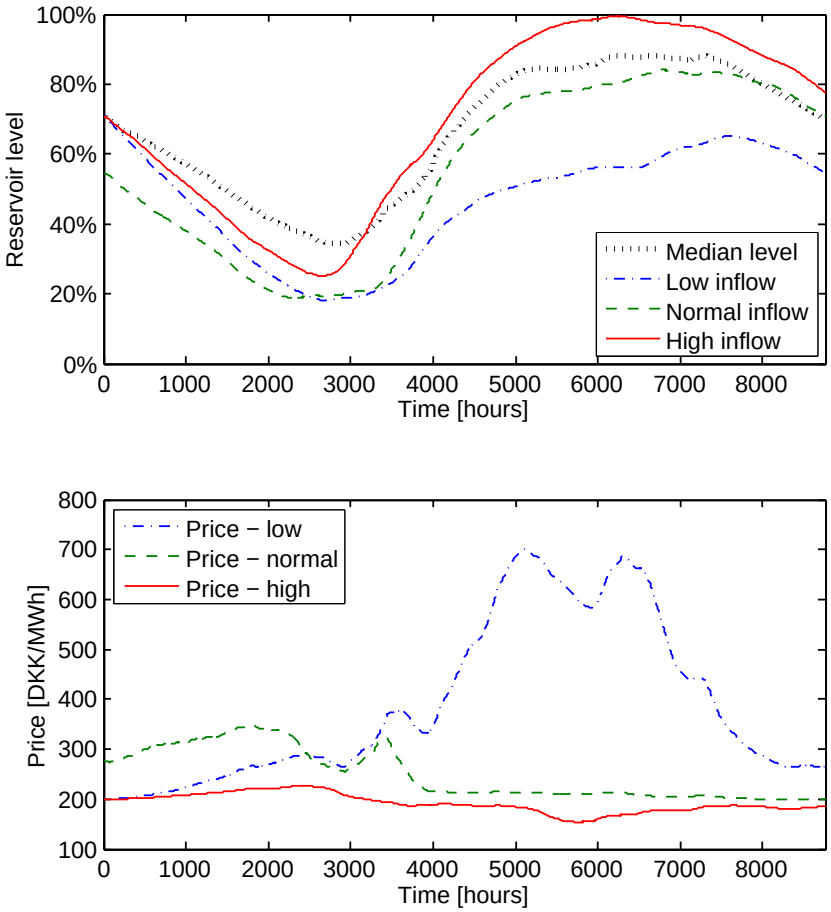

Figure 4.9: The upper diagram depicts the hydro reservoir level in Norway for three different inflow series together with the real historical median reservoir level. The lower diagram shows the corresponding prices.

gian and Swedish hydro reservoirs for balancing purposes may prove to be valuable. A study from Norway concludes that integrating wind power into hydro production scheduling raises the value of wind power [31].

4.2.1 Monte-Carlo simulation

To analyse the impact of wind power on power prices in Denmark West a monte-carlo analysis was used. For each simulation the installed wind power capacity was held constant, and random hydro inflow series and random load, wind, and decentral CHP series were drawn for each run. Each simulation consisted of 25 runs, which when considered together, gave a distribution of possible outcomes for the wind power level in question. This process was

then repeated for each level of installed wind power capacity desired.

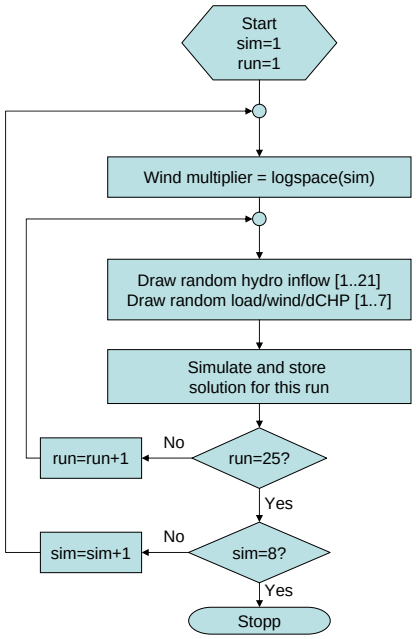

Figure 4.10: Procedure for analysing the impact of wind power on power prices.

The installed wind power capacity at the end of 2006 was taken as the reference level, see table 4.1 for numbers. To set the installed capacity of wind power at a higher level, the historical power output was multiplied by a factor greater than one. This approach assumes that the volatility in wind power output is unaffected by growth in installed capacity as detailed in section 2.2.3.

Table 4.1: Approximate numbers for wind power in 2006 equal to a factor of 1.

	Denmark	*Germany*
Installed capacity	3100MW	19000MW
Energy output	5TWh	35TWh
% of demand covered	15%–19%	6%

Eight logarithmically spaced wind multiplication factors were used:

$$factor \in [1.0,\ 1.3895,\ 1.9307,\ 2.6827,\ 3.7276,\ 5.1795,\ 7.1969,\ 10.0] \quad (4.1)$$

Where a factor of 1 is the 2006-level and 2.68 corresponds to between 40% and 50% of energy demand covered by wind power in Denmark. Installed

wind power capacity in all areas, not only Denmark West, was multiplied by the same factor. The entire procedure is illustrated in figure 4.10.

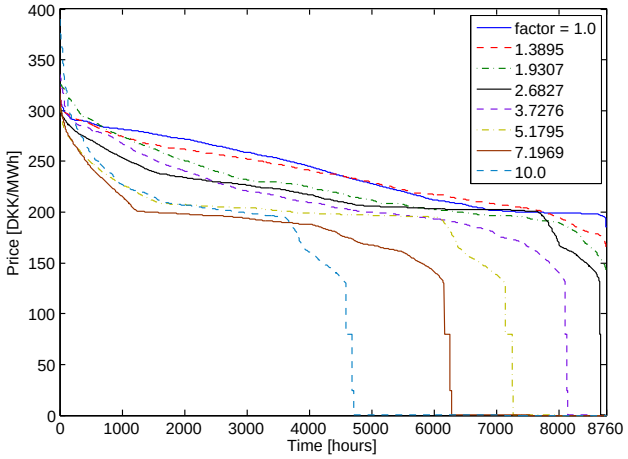

Figure 4.11: Median duration curves for all simulations drawn from figure 4.12.

Results are shown in figure 4.12 and the medians of all simulations are superimposed on one another in figure 4.11. Table 4.2 lists the average price for each factor, the standard deviation of hourly price variations, and the reduction in price relative to the 2006 level. Results reveal that a considerable increase in wind power capacity is needed before prices drop significantly. There is a threshold at a factor of 2.7, above which wind power becomes the marginal producer in a noticeable number of hours. Further expansions above this level leads to overflow of wind energy during more hours and frequent bottlenecks on tie-lines as the export capacity becomes strained.

The power market model is based on two important assumptions that help explain the moderate impact of wind power on power prices. First, the model assumes perfect competition and markets that are very efficient. At present not all generators part-take in the spot market and are unable to react to price signals given by the market. The power exchange NordPool states that 176TWh was traded at the physical market during 2005. At the same time, consumption in the NordPool area was 393.9TWh. The spot markets of central Europe are even less liquid; further development and integration of the markets are important to accommodate high shares of wind power.

Second, the model also assumes that all cross-border transfer capacity can be utilized for spot trade. This is often not true in the real power system: Transfer capacities can be reduced for a number of reasons like network failures, internal congestions, and a constrained regional power balance. A higher share of wind power will probably worsen the situation for two rea-

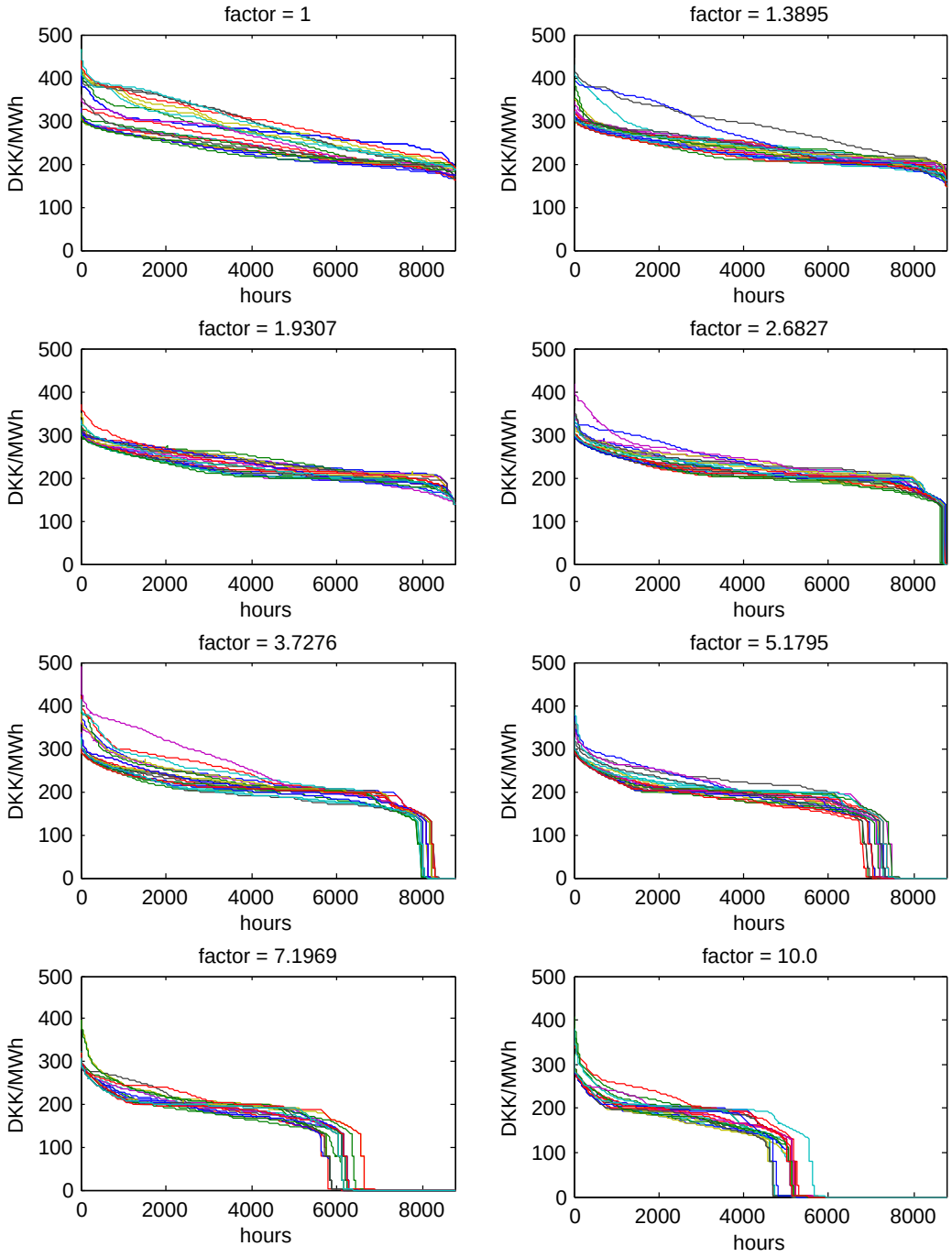

Figure 4.12: Results from the monte-carlo simulation. Each diagram shows the result of one simulation with 25 runs. A factor of 1 refers to the level of installed wind power capacity in 2006.

Table 4.2: Average power price and standard deviation as a function of the wind power multiplication factor.

Factor	*Mean* [DKK/MWh]	*std.dev.* [DKK/MWh]	*% reduction*
1.0	253.8	43.78	–
1.3895	237.6	35.32	6.40%
1.9307	225.6	31.73	11.08%
2.6827	218.1	37.59	14.05%
3.7276	200.4	68.51	21.02%
5.1795	165.8	83.67	34.66%
7.1969	138.1	94.78	45.60%
10.0	110.4	99.25	56.51%

sons. First, forecasts of wind power generation are always associated with some uncertainty, and transfer capacity may have to be reserved for regulating purposes. Second, wind power is often located at remote sites. This can lead to constrained power balances and internal bottlenecks. Presently, spot trade is conducted one day ahead of the physical delivery. Trading spot closer to the physical hour (e.g. hour-ahead instead of day-ahead) can help alleviate the situation, as uncertainty in wind forecasts decrease closer to the actual hour [32].

Wind turbine owners income

As discussed in section 2.2.3, assuming zero marginal cost of wind power can result in very low income to wind turbine owners at high levels of wind power penetration. Consequently, such a situation is unrealistic because investments would have ceased before reaching that far. Figure 4.13 depicts the average income per MWh and the total income from power sales to the wind power industry in Denmark West, as a function of installed wind power capacity.

The specific income naturally decreases monotonically as the installed wind power increases. Total income to the industry peaks at a factor somewhere between 2.68 and 3.73. How much capacity that will be installed depends on the investment cost and government subventions. Rising fuel costs and carbon taxes might also help offset the income reduction by raising the marginal cost of thermal power, see section 4.2.2 below. However, it seems unlikely that capital will be allocated to install capacity to cover more

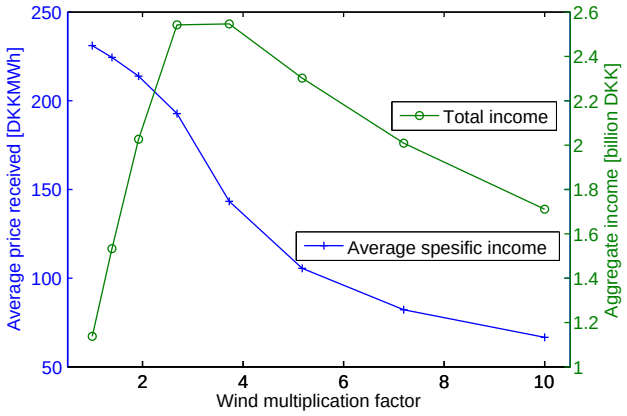

Figure 4.13: Income to wind turbine owners in Denmark West as a function of the installed capacity (wind power multiplication factor).

than around 50% of energy demand with present prices.

The income will also be affected by the uncertainty in wind forecasts, however, this has not been accounted for here. With a long delay between the physical delivery of energy and the time of trade, prediction error of wind power will be significant. This leads to large quantities traded at the balancing market, at lower profit for the wind turbine owner.

4.2.2 Sensitivity to thermal generation costs

Relatively modest thermal generation costs have been used in the model. In the 2006 World Energy Outlook, the International Energy Agency states that it "expects that crude oil and refined-product markets remain tight" [33]. The threat of severe supply disruption and price shocks is also stressed. This indicates that the cost of thermal generation will rise in the next decades compared to the cost assumed in the model.

Figure 4.14 depicts the change in average electricity price as a function of thermal generation costs. The dotted diagonal line represents a system with only thermal generation where an increase in costs is transfered to the electricity price in a 1:1 relationship. A system with a mix of renewables and thermal generation capacity has a less steep slope; the higher the share of renewables, in this case wind power, the smaller the angle of inclination. In the figure, the lines represent shares of wind power corresponding to factors as defined by equation 4.1.

As is expected, a system with much wind power is less prone to high thermal generation costs, but the share of wind power must be quite large to make an impact. At a factor of 2.68 the increase in the electricity price,

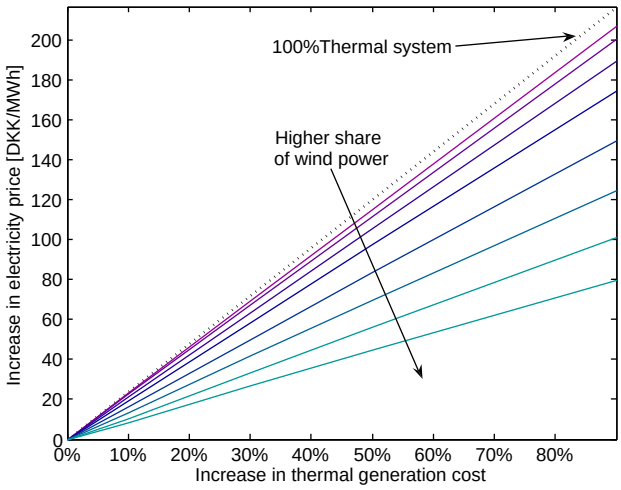

Figure 4.14: Impact of thermal generation costs on the average electricity price for different wind multiplication factors.

resulting from a thermal generation cost increase, is reduced by 16%, and at a factor of 10 it is reduced by 62%.

Impact on wind turbine owners income

Rising thermal generation costs will also impact on the income to wind turbine owners. Figure 4.15 depicts the sensitivity in wind turbine owners income to increased generation costs and is analogous to figure 4.13. Higher thermal generation costs result in higher income to wind turbine owners, but the total aggregate income still peaks at a factor between 2.68 and 3.73. With a 50% increase in thermal generation costs, the market could sustain 3.25 times as much installed wind power capacity as today without a reduction in income to wind turbine owners. That equals approximately 10TWh installed capacity or 50%–60% share of domestic energy consumption in Denmark. Even a 10% increase in thermal generation costs can offset the negative impact on wind turbine owners income from a doubling of the installed capacity.

The implication of this is that possible high fuel prices or carbon dioxide abatement costs can allow for very high shares of wind power in the system and still retain a reasonable income to wind turbine owners.

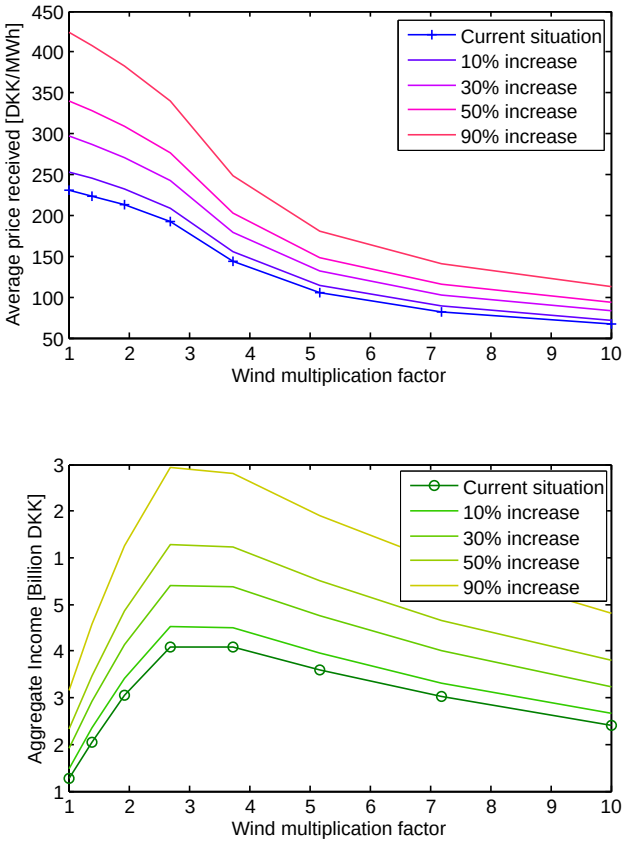

Figure 4.15: Thermal generation costs and the impact on wind turbine owners income.

4.2.3 Sensitivity to transfer capacity

If the transfer capacity on cross-border tie-lines has to be reserved for regulating purposes, or on the other hand, the capacity is expanded to better integrate the markets, prices will change.

Figure 4.16 shows the sensitivity to a global change in the cross-border transfer capacity. By a global change it is meant that the capacity on all tie-lines is scaled up or down by the same factor. The simulation was done for the median scenario with a wind multiplication factor of 2.68 and reveals that lower capacity leads to higher volatility and vice versa. Although average prices remain relatively constant there is a great downside for wind turbine owners if the capacity is reduced. With a 50% reduction in transfer capacity, the income is slashed by more than 30%. On the contrary, income only rises by 10% if the transfer constraints are relaxed by 50%. Thus, to enable a large share of wind energy in Denmark, transfer capacity can not be reserved for

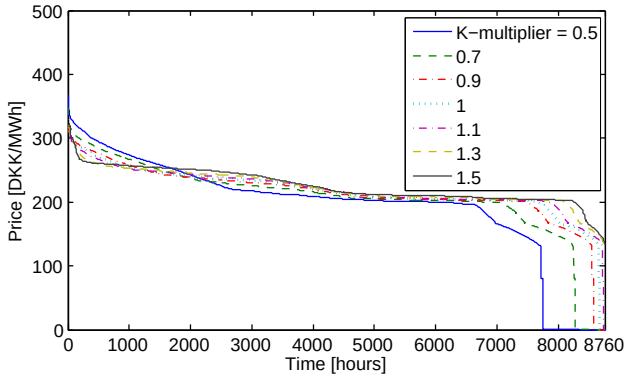

Figure 4.16: Sensitivity to variation in the cross-border transfer capacity.

regulating purposes; else the income potential will be too limited and new wind power investments unprofitable.

4.2.4 Sensitivity to hydro inflow

The price in Denmark is dependent on hydro inflow to the reservoirs in Norway and Sweden. Figure 4.17 shows a duration diagram of the price for the average inflow and lines to mark a 95% confidence interval. High inflow nat-

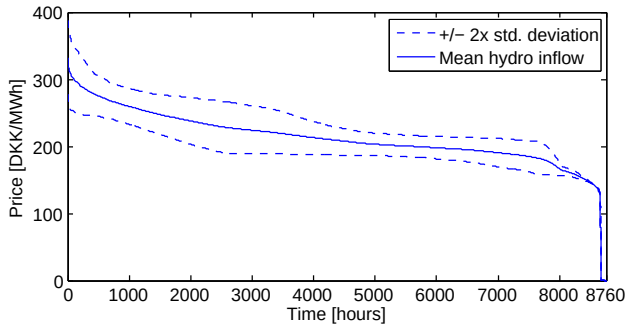

Figure 4.17: Sensitivity to variation in hydro inflow with a wind multiplication facto of 2.68.

urally lowers the price and vice versa. Again, the simulation was done for the median price series using a wind multiplication factor of 2.68.

4.2.5 The balancing role of Norwegian hydro power

Hydro and wind energy have complimentary characteristics, the first storable, the other intermittent. Therefore it is of interest to examine how much the

Norwegian hydro reservoirs help balance out the fluctuating wind energy in Denmark. Three scenarios were investigated by modifying the model slightly.

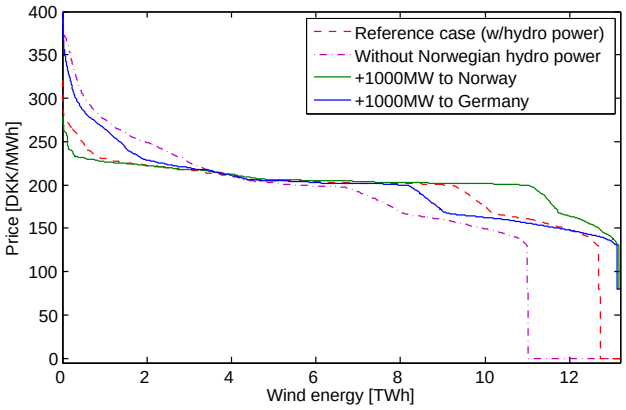

Figure 4.18: Income duration curves for wind power in Denmark West in a single year with wind power multiplication factor of 2.68.

The following describes the departure from the original model for each of the three scenarios:

1. Norwegian hydro power was "removed" from the system by setting all transfer capacity to and from Norway equal to zero.

2. The tie-line from Denmark West to Norway was increased by 1000MW, keeping all other tie-lines at normal levels.

3. The tie-line from Denmark West to Germany was increased by 1000MW, keeping all other tie-lines at normal levels (also the ones connecting Norway).

These cases were compared to the system as it is today. For all four cases a wind power multiplication factor of 2.68 was used to amplify the results.

Figure 4.18 shows wind power income duration curves for the four scenarios. Without Norwegian hydro power, there would be greater variation in income from wind power sales, and total income would drop by 10% because the export capacity becomes limited during high wind periods. On the other hand, expanding the capacity of the tie-line to Norway by 1000MW would greatly reduce volatility and stabilize income at a somewhat higher level than the reference case. Expanding the tie-line to Germany by 1000MW would also increase total income, but result in greater intra-year volatility.

For the particular case presented in figure 4.18, the hydro reservoirs in Norway give an added value of 260 million DKK per year to wind turbine

owners in Denmark West. The benefit is due to higher prices during high wind speed hours. At the same time, it reduces peak prices enough to keep average spot prices below the level without hydro power. Expanding the capacity to Norway by 1000MW gives an additional added value of 140 million DKK per year to wind turbine owners and further lowers the average spot price. Thus Norwegian hydro power benefits both consumers and wind turbine owners. On the other hand, expansion of capacity to Germany gives an added value of 85 million DKK per year, mainly due to higher peak prices. Thus, a stronger link to Germany results in higher spot prices and lower consumer benefit.

4.3 Final remarks

In this part of the report, a simple and flexible power market model has been developed. Focus has been on power prices in Denmark West. The model was tested and proved to produce plausible results both for extreme inputs and normal operating conditions. Comparison of simulated prices to historical prices revealed too low volatility which indicates that the simulated market is more stable than the real market. In turn, this may imply that the various effects studied will be amplified in real life.

Simulation of Danish power prices indicates that prices will fall, and volatility increase, with a greater share of wind power. However, the effect is relatively moderate; wind power does not become the marginal producer until the installed capacity reaches about 8300MW in Denmark. This result hinges on efficient and integrated power markets across Europe, and technical solutions that allow capacity on cross-border tie-lines to be used for spot trade and not to be reserved for regulating and reserve purposes. If such solutions can not be found, the impact of wind power will become evident at a lower level than predicted in this study.

A high share of wind power leads to less consumer expenditure on electricity. Estimates show that consumers in Denmark West saved 12.5% on their power bill in 2005 due to wind power. This result falls in line with one previous study.

Because wind power has almost zero marginal cost, a high share of wind power may pose economic difficulties for wind turbine owners. In absence of government subventions or price coordination among wind turbine owners, prices will fall to zero when wind power becomes the marginal generator. In turn, this leads to reduced income and possible problems in covering capital costs. The income reduction can to a great extent be alleviated through higher fossil fuel prices or a tax leading to higher thermal generation costs. With a 50% increase in thermal generation costs, the installed wind power

capacity could be more than trippled and still retain the same income to wind turbine owners as today.

Utilizing the hydro reservoirs in Norway to balance out fluctuations in wind energy greatly stabilises the power price in Denmark West and secures income to wind turbine owners. In a possible future Danish power market with a 50% share of wind energy, it gives an added value of about 10% to wind power. The value can be increased by further expanding the tie-line capacity to Norway. Expansion of the tie-line capacity to Germany will also help secure income to wind turbine owners, but new capacity to Norway is preferable.

Part II

Case, electrolytic hydrogen production

Chapter 5

Introduction

Increased generation of electricity from wind power in Denmark has lead to more volatile electricity prices, and in periods of high wind speed, prices can become very low. At the same time, the market for hydrogen is growing rapidly, mostly fueled by increased demand for fertilizer and the shift to heavier crude oils in oil refining that demand more hydrogen for cracking. This has lead to renewed interest in water electrolysis because new electrolysers are able to ramp up and down production quickly and take advantage of volatile electricity prices.

Part I investigated the impact of increased wind power penetration in Northern Europe on power prices in Denmark-West. Results showed that a moderate increase in volatility and reduction of prices can be expected. In preliminary work to this master thesis, the author together with Magnus H. Strømmen developed models to analyse the profitability, dimensioning, and operation of an electrolyser [3]. A modified version of these models will be used with results from part I to investigate how electrolyser costs are affected by increased wind power penetration. The following gives a brief summary of the relevant model developed in [3] before presenting results of the analysis.

Chapter 6

Problem definition

The problem of this part is to calculate the cost of electrolysis on the basis of a year of simulated electricity prices. To calculate the cost of electrolysis, both the operation and investment strategy must be optimized. In this chapter, the dimensioning and operation of an electrolyser with a hydrogen storage connected to a customer requiring a constant flow of hydrogen through a pipeline, is analysed.

There are two types of decisions to be taken: (1) The size of the electrolyser and storage to build and (2) how much hydrogen to produce for every hour given the electricity price. A larger electrolyser and storage allows a greater share of production during off-peak hours at the cost of more capital expenditure. The decisions taken should maximize net present value of the project which is equal to minimizing costs since the revenue cannot be influenced.

6.1 Operation and investment optimization

Optimization of the problem can be split into two sub-problems. First, an operation strategy to minimize production costs given knowledge about prices for a given number of hours into the future. Second, an investment strategy to determine the size of the electrolyser and storage given the optimal operation strategy.

6.1.1 Sliding horizon operation strategy

Given excess electrolyser capacity and a storage, it is optimal to produce more during hours with low electricity prices and avoid production in the most expensive peak-hours. The challenge is to meet the requirement of

Table 6.1: Notation used in formulation of the optimization problem

Symbol	*Description*
Q_t	Power (MW) bought during time step t in the spot market for electricity.
T	Horizon length in hours.
D	Required delivery of hydrogen (Nm^3/h).
E	Electrolyser capacity (MW).
K	Compressor size (Nm^3/h).
S	Storage size (Nm^3).
S_0	Hydrogen in storage at beginning of period (Nm^3/h).
P_t	Hourly electricity spot prices (DKK/MWh).
η	Efficiency of electrolyser (Nm^3/MWh).
$o(t_0)$	Operation costs for the period of T hours starting at t_0 [DKK]

constant delivery at the least possible cost. For a period of T hours, starting at t_0, the following formulation describes the problem:

$$\min o(t_0) = \min \sum_{t=t_0}^{t_0+T} (P_t Q_t) \tag{6.1}$$

$$s.t. \quad 0 \leq Q_t \leq E \tag{6.2}$$

$$s.t. \quad 0 \leq S_0 + \sum_{t=t_0}^{t'} (\eta Q_t - D) \leq S \quad \forall\ t' = [t_0, t_0 + 1 \ldots t_0 + T] \tag{6.3}$$

Constants E, D, and S are given, and electricity spot prices P_t are assumed to be known for all $[t_0 \ldots t_0 + T]$ hours. Additionally a compressor of size K is needed to compress hydrogen for storage. The following equation apply:

$$K = \eta E - D \tag{6.4}$$

To simulate operation, the problem in 6.1 is solved for a set number of hours T, called the *horizon*, then the algorithm moves one step with length $T/2$ forward (i.e. t_0 is incremented by $T/2$) and solves the problem again. This is repeated for the whole time series and assumes that prices T hours into the future are known with certainty.

Computation time increases rapidly with a long horizon because the number of constraints grow proportionate to T, as can be seen from equation 6.3. However, for a relatively short horizon the strategy is efficient.

6.1.2 Investment and capacity optimization

Before investing in an electrolyser plant, sizing of the electrolyser, storage, and compressor to minimize present value (PV) of the total costs must be carried out. A relatively large electrolyser has been analysed; thus investment costs have been kept proportional to capacity, but any other relationship could easily be implemented.

To determine the optimal combination of storage and electrolyser size, a constrained nonlinear solver – with storage size, S, and electrolyser capacity, E, as variables – was used. The value to be minimized was computed as the PV of the sum of operation costs and investment costs for the whole lifetime of the plant. The operation costs were calculated by solving the operation sub-problem in equation 6.1, given S and E. In effect, the optimization tries several combinations of S and E until the optimal combination is found.

The nonlinearity of the problem arises because the operation cost must be calculated iteratively. I.e., the operation cost for hours t_0 to $t_0 + T$ can only be found when the operation prior to t_0 has been determined. So even though all sub-problems are linear both in constraints and object function, it is not possible to formulate the entire investment and capacity optimization as one linear problem.

Chapter 7

Results

The first section of this chapter deals with the selection of horizon length. An example of operation is also shown to verify that the algorithm works as expected. Section 7.2 presents results from the analysis of how wind power affects the cost of hydrogen production by electrolysis.

Input to the analysis was time series of hourly simulated power prices for Denmark West produced by the model from part I. To study the effect of wind power on hydrogen production cost, the optimization was rerun several times. For each run, the input-prices corresponded to a different share of installed wind power capacity. The same procedure was done to investigate the impact of thermal generation costs.

In the following, the number of *demand hours* is used to describe the size of the storage, and the electrolyser size is give as a *multiple of demand per hour*. Thus 1 demand hour is the volume (in Nm^3) sufficient to cover demand for one full hour, and an electrolyser size of 1 is the capacity (in Nm^3/h) that is necessary to cover exactly the demanded volume flow.

7.1 Verification

7.1.1 Determination of horizon length

Before analysing the cost of electrolysis, it was essential to determine a horizon length. To see how long horizon was necessary to take advantage of the flexibility provided by a storage, operation was simulated using different horizon lengths and different storage sizes with ample electrolyser size. Results are shown in figure 7.1. As is expected, a longer horizon is needed to plan for larger storages; the shortest horizon length needed to realize full cost reductions is typically about four times the storage size (given in demand hours).

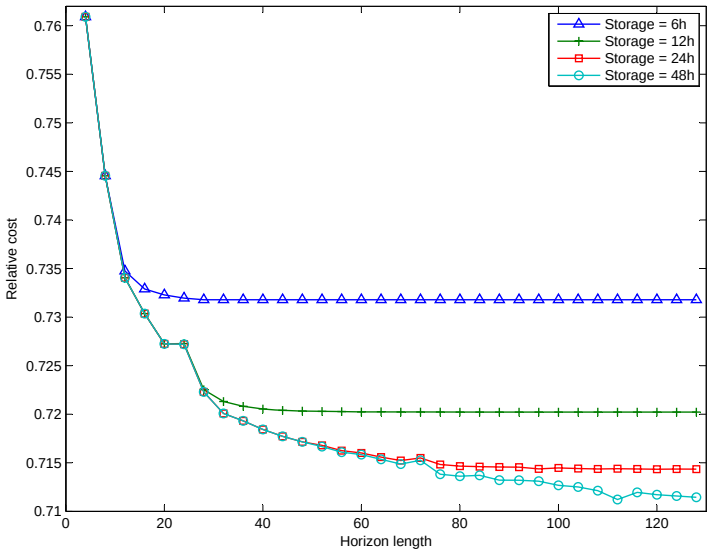

Figure 7.1: Production cost savings for different horizon lengths and storage sizes. The cost of storage is not taken into account. Source [3].

Because electricity prices show a strong tendency of mean reversion and cyclical patterns, planning ahead for a very long time does not give any additional benefits. It is better to fill and empty the storage on these cycles, and thus it suffices to plan some cycles ahead. Figure 7.1 shows that costs have a tendency to decay exponentially with increased horizon length and approach some level of cost reduction asymptotically.

A horizon length of 48 hours was selected for the rest of the simulations. This provides good enough cost reductions for storages up to 48 demand hours without being too unrealistic in terms of forecasting accuracy.

7.1.2 Example of operation

Figure 7.2 shows normalized electricity price, production, and storage levels in a representative 168-hour period. One can see that the algorithm performs as expected; it mostly produces during off-peak hours and empties the storage during peak hours.

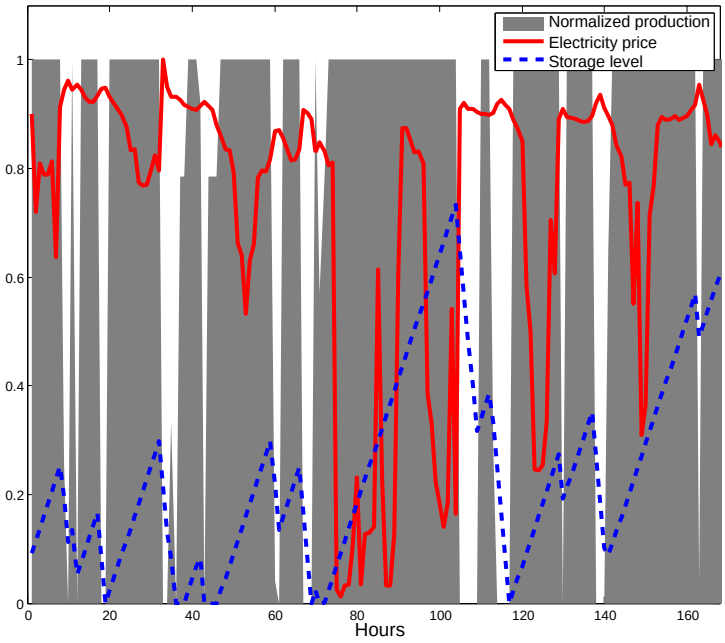

Figure 7.2: Normalized production and storage level in a representative week. Source [3]

7.2 Impact of increased wind power penetration on electrolyser cost

In this section, the cost of producing hydrogen by electrolysis and by steam methane reforming (SMR) are compared. The reason behind selecting SMR as a reference is because it is the cheapest and most common way of producing hydrogen today.

When deciding to build a plant to produce hydrogen, the investment costs have to be taken into account. If, in the long run, hydrogen is sold at a price so low as not to cover both investment costs and variable costs, the plant will have to be shut down. Thus, unless otherwise specified, when costs are compared in this section the *long term marginal costs* are meant. I.e., the total cost of producing hydrogen including capital expenditure.

Key assumptions needed to calculate the cost of large scale hydrogen production by electrolysis and by SMR are summarized in table 7.1. All assumptions equal those detailed in [3] apart from the electrolyser efficiency which has been reduced to 4.85kWh/Nm^3. The capital cost of the electrolyser is a ballpark estimate for a large-scale electrolyser (>800 Nm^3/h). In addition to operation and maintenance cost, the electrolyser cells have to be replaced

Table 7.1: Assumptions for electrolysis and steam methane reforming (SMR).

Description	*Assumption*
Electrolyser capex	11862 DKK/Nm^3/h
Storage capex (200 bar, underground lined rock cavern)	5909 DKK/m^3
Compressor capex	2627 DKK/Nm^3/h
Lifetime of electrolyser	40 years
Discount rate	8%
Yearly electrolyser O&M in % of capex	1%
Energy efficiency of electrolyser	4.85 kWh/Nm^3/h
Fixed cost of SMR	0.182 DKK/Nm^3
Variable cost of SMR (Corresponding to nat. gas. price of 140 DKK/Sm^3)	0.714 DKK/Nm^3

every 10 years at a cost equal to 30% of the electrolyser capex. Both the price of natural gas used in SMR and the price of electricity used in electrolysis are without taxes and transmission fees, and it is assumed that the necessary infrastructure (natural gas pipelines, electricity grid) is available and can be freely used. It should also be noted that the storage costs are based on the cost of underground steel lined rock caverns which is much cheaper than steel tanks. In calculating the volume needed to store hydrogen at 200 bar it was assumed that hydrogen is an ideal gas at constant temperature, thus volume is inversely proportinal to pressure.

Figure 7.3 shows the normalized variable cost of hydrogen production by electrolysis as a function of the *wind power multiplication factor* (see section 4.2.1). Additionally, the normalized average electricity price is plotted for comparison. The operation cost shown includes excess investment costs for electrolyser, storage, and compressor above the minimum needed to cover demand. The minimum investment cost does not provide any flexibility, it implies that an electrolyser to cover the exact demand is installed and no storage is built. Money spent at capacity exceeding this must be regained by flexible operation.

One can see that the operation cost of electrolysis declines in line with the average electricity price until a factor of about 7. This means that little additional savings can be gained from flexible operation until the installed wind power capacity becomes very high. Part of the reason for this is that the price model from part I generates prices with too little volatility, thus gains from flexible operation become small. In this manner, the relative gains

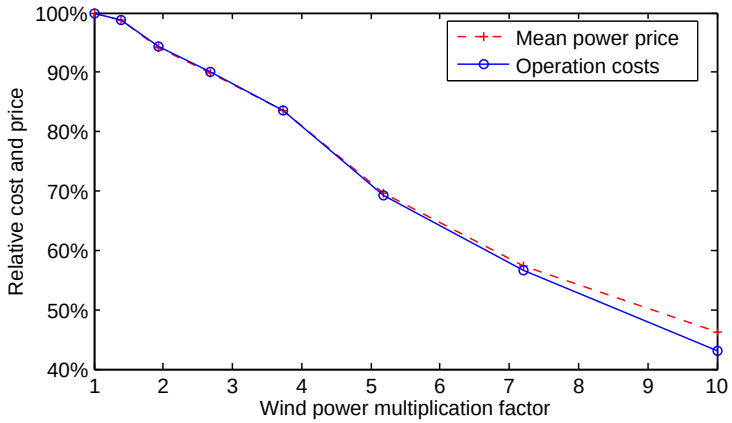

Figure 7.3: Relative operation costs and mean power price as a function of installed wind power capacity.

can be regarded as a lower bound.

An example of the possible gains from installing excess electrolyser capacity and storage is provided in figure 7.4.The surface consist of the net savings from flexible operation given different electrolyser and storage sizes for a wind power multiplication factor of 5.18. The optimal combination for this case is storage for approximately 10 hours and an electrolyser capacity of 120%. Resulting savings amount to only 0.01 DKK/Nm^3, or a little less

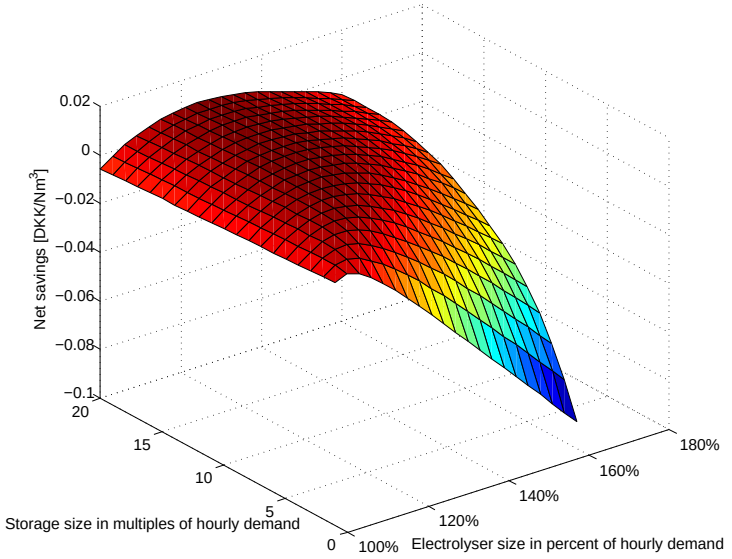

Figure 7.4: Net savings from flexible operation as a function of installed electrolyser and storage capacity. The wind power multiplication factor is 5.18.

than 1% of production costs.

Even though the gains from flexible operation are low, production costs do fall as the installed wind power capacity increases. Figure 7.5 depicts the production cost of hydrogen (including capital expenditure on storage, compressor, and electrolyser) compared to the equivalent cost of steam methane reforming (SMR). With the present level of installed wind power capacity, simulation results indicate that electrolysis is 47% more expensive than SMR. As the installed wind power in the system increases, the cost of electrolysis falls, but the cost of SMR remains constant because it is dependent on natural gas costs. At a factor of 5.8, corresponding to approximately 100% wind energy in Denmark, electrolysis breaks even with SMR.

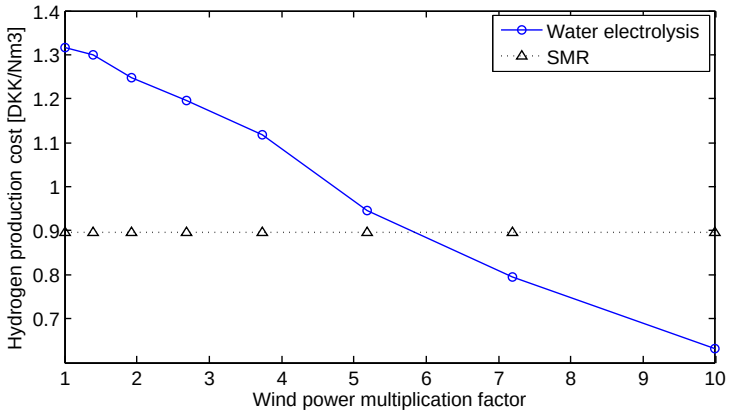

Figure 7.5: Hydrogen production cost by electrolysis and SMR. For conversion to kg use: 1 kg=11.14 Nm^3.

7.2.1 Sensitivity to thermal generation costs

When natural gas prices rise, the cost of SMR will increase. Since natural gas is a common fuel in electricity generation, and the price of fossil fuels are tightly correlated, electricity prices will also rise. The following analysis assumes that thermal generation has the same relative increase in costs as natural gas, i.e., if the natural gas price doubles, the marginal cost of all thermal generators double.

For a power system that relies only on fossil fuels, an increase in fuel prices will be transfered to the electricity price in its entirety (see figure 4.14). Since electrolysis is less capital intensive than SMR, the cost of hydrogen produced by electrolysis is more sensitive to an increase in thermal generation costs. The hydrogen cost by SMR is comprised of ≈25% capex whereas the same

number for electrolysis is ≈10%. For example if the electricity price and the natural gas price both increased by 20%, the cost of producing hydrogen by SMR would increase by 15%, but the cost of producing hydrogen by electrolysis would increase by 18%. With the present share of renewables, there is almost always a thermal generator that is the price setter; consequently, an increase in fossile fuel prices can not be expected to improve the competitive ability of an electrolyser.

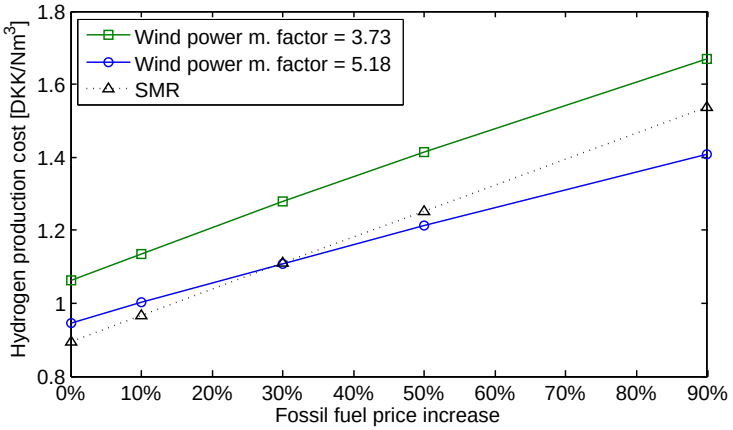

Figure 7.6: Sensitivity of hydrogen production cost, by SMR and electrolysis, to increased fossil fuel prices. The wind power multiplication factor is 5.18.

However, if wind power becomes dominant in the power system, higher fossil fuel prices will only partially lead to increased electricity prices. Figure 7.6 shows the sensitivity of hydrogen production costs to increased fossil fuel prices, or identically higher thermal generation costs.

For a wind power multiplication factor of 5.18, the comparative advantage of electrolysis becomes better as the cost of fossil fuels increase; eventually, electrolysis becomes the cheaper way of producing hydrogen. For a wind power multiplication factor of 3.73, the slopes are almost identical, and the comparative advantage stays the same. Accordingly, it is only possible for water electrolysis to outperform SMR as *the* way of producing hydrogen in a power system with a very high share of renewables like wind power.

It should be noted that savings from flexible operation increases more than tenfold when the thermal generation costs increase by 90%. Figure 7.7 depicts the equivalent of figure 7.4, but with thermal generation costs increased by 90%. The optimal electrolyser size is 180% of demand, and the optimal storage size is 22 demand hours. Total savings amount to 0.126 DKK/Nm^3, 12 times as much in figure 7.4.

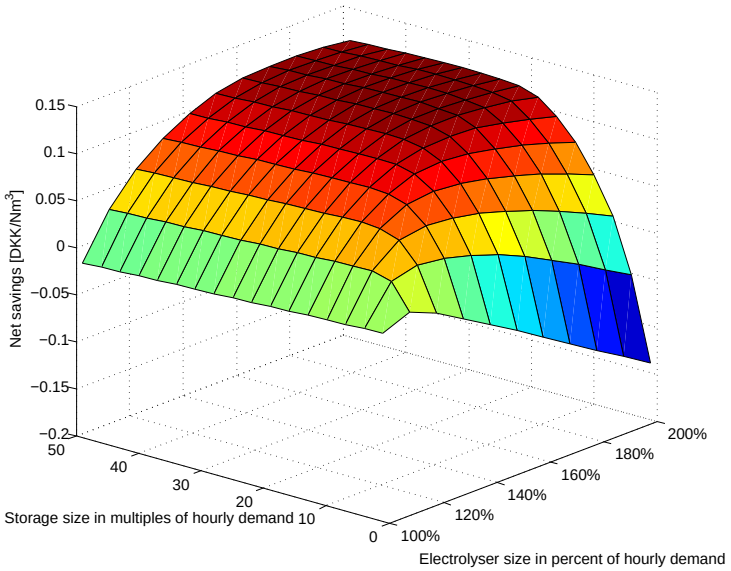

Figure 7.7: Net savings from flexible operation as a function of installed electrolyser and storage capacity. The wind power multiplication factor is 5.18 and thermal generation costs are increased by 90%.

7.2.2 Variable delivery

In some cases it is not necessary to deliver a constant amount of hydrogen. If so, the problem is mathematically essentially the same as in equation 6.1, but with zero cost of storage and compression. The problem is still to buy electricity during low price hours and invest in electrolyser capacity such that the marginal benefit of expanding the electrolyser capacity equals the marginal production cost. However, prices can not be known with certainty beforehand, and some kind of rolling planning will have to be employed. Because of the relaxed constraints on operation and the lower investment costs, such a configuration will inevitably come at a lower total cost per unit of hydrogen produced. Results from [3] indicates that this difference is about 5% and presently not enough to tip the scales in favor of electrolysis.

7.3 Concluding remarks

The cost of large scale hydrogen production by water electrolysis in Denmark West has been analysed. The hypothesis was that electrolysis can become cheaper than steam methane reforming (SMR) because electricity prices will drop and become more volatile if the wind power penetration in Europe increases.

Results indicate that a very high share of wind energy is needed before electrolysis breaks even with SMR. Five to six times the present level of installed wind power capacity in Denmark is necessary. This corresponds to 100% wind energy in Denmark. Additionally, the study assumes a high share of wind energy in Germany.

Higher natural gas prices contribute little to the comparative advantage of electrolysis at wind power penetrations below 60–70%. The reason being that higher fossil fuel prices largely are transferred to the electricity price. A 30% higher natural gas price can make electrolysis break even at a wind power penetration of about 85% in Denmark.

With storage and excess electrolyser capacity it is possible to produce more hydrogen during hours with low electricity prices. Optimization of storage size and electrolyser capacity shows that, presently, only small gains can be achieved from such flexible operation. However, if a combination of high wind power penetration and a high natural gas price is reached, large gains can be made from flexible operation.

Several factors may alter the level of wind power at which electrolysis breaks even with SMR. Some of the most important factors are: (1) The electricity prices used in this study demonstrate too low volatility, thus gains from flexible operation are somewhat undervalued. (2) By bidding on the regulating market for electricity, extra income can be realised (see [3]). (3) If Denmark further strengthens its power lines to neighbouring countries, the impact of wind power can be greatly reduced. This keeps electricity prices and costs high, even in high wind speed hours. (4) High shares of wind power may lead to cross-border transmission capacity being reserved for regulating purposes. This will increase the impact of wind power, result in lower electricity prices during high wind speed hours, and reduce electrolyser costs. (5) The results depend on a relatively inexpensive underground storage solution. If more expensive storage solutions must be used, gains from flexible operation will diminish. (6) If hydrogen is required in a place where infrastructure for gas lacks, but electrical power is available, the numbers will look different. (7) If the delivery of hydrogen can be variable, such that no storage is needed for flexible operation, about 5% cost reductions can be realised. It also improves the possibility of gains from the regulating market.

If several of these factor pull together, electrolysis can become profitable at lower wind power penetrations than this report shows. If the target of 50% wind energy in Denmark is reached, it might be necessary to reexamine the situation. However, it seems safe to say that SMR will remain the least expensive option for large scale hydrogen production until then.

To sum up, this study indicates that for electrolysis to break even with SMR, the following conditions must apply: Wind power penetration above

85% in Denmark, increased natural gas price by 30% or more, inexpensive hydrogen storage solution and no expansion of electricity transmission capacity from Denmark West to neighbouring countries.

Bibliography

[1] European Wind Energy Association (EWEA). *Wind Power Targets for Europe*, October 2003.

[2] Energinet.dk. Udtræk af markedsdata (eng.: Market data download). `http://www.energinet.dk/da/menu/Marked/Udtr\%c3\%a6k+af+markedsdata/Udtr\%c3\%a6k+af+markedsdata.htm`.

[3] M. H. Strømmen and T. Trötscher. Profitability Assessment of a Grid Connected Electrolyser, 2006. Preliminary work to the Master Thesis at the Norwegian University of Science and Technology.

[4] P. A. Østergaard. Ancillary services and the integration of substantial quantities of wind power. *Applied Energy*, 83(5):451–463, 2006.

[5] V. Akhmatov and H. Knudsen. Large penetration of wind and dispersed generation into Danish power grid. *Electric Power Systems Research*, 77(9):1228–1238, 2007.

[6] H. Lund. Large-scale integration of wind power into different energy systems. *Energy*, 30(13):2402–2412, 2005.

[7] H. Holttinen. Impact of hourly wind power variations on the system operation in the nordic countries. *Wind Energy*, 8(2):197–218, 2005.

[8] H. Brand, C. Weber, P. Meibom, R. Barth, and D. J. Swider. A stochastic Energy Market Model for Evaluating the Integration of Wind Energy. In *Proceedings of the 6th IAEE European Conference on Modelling in Energy Economics and Policy*, 2004.

[9] PE Morthorst. Wind power and the conditions at a liberalized power market. *Wind Energy*, 6(3):297–308, 2003.

[10] H. Holttinen, K.O. Vogstad, A. Botterud, and R. Hirvonen. Effects of Large-Scale Wind Power production on the Nordic Electricity Market.

In *Proceedings of European Wind Energy Conference, EWEC*, pages 2–6, July 2001.

[11] Sintef Energy Research. Hydro-thermal operation and expansion planning. `http://www.sintef.no/content/page1____4941.aspx`.

[12] Union for the Co-ordination of Transmission of Electricity. *System Adequacy Retrospect 2005*, 2005.

[13] Organization for cooperation of Nordic transmission system operators (NORDEL). *Nordel Annual statistics*, 2005.

[14] M. J. J. Scheepers, A. F. Wals, and F. A. M. Rijkers. Position of large power producers on electricity markets of north western europe. Technical Report ECN–C–03–003, Energy research Centre of the Netherlands, 2003.

[15] O. B. Fosso, A. Gjelsvik, A. Haugstad, B. Mo, and I. Wangensteen. Generation scheduling in a deregulated system. The Norwegian case. *Power Systems, IEEE Transactions on*, 14(1):75–81, 1999.

[16] J. D. Sterman. *Business Dynamics*. Mc Graw Hill, 2000.

[17] P. Nørgaard and H. Holttinen. A multi-turbine power curve approach. In *Proceedings of Nordic Wind Power Conference*, 2004.

[18] J. Cappelen. Månedens vejr Oktober 1998 - juli 2003 (en.: Monthly weather reports okt. 1998 - jul 2003). Technical Report 03-31, Danmarks Meteorologiske Institut, 2003.

[19] Danmarks Meteorologiske Institut. Månedens vejr (en.: Monthly weather reports). `http://www.dmi.dk/dmi/index/danmark/oversigter/maanedens\_vejr\_-\_oversigt.htm`.

[20] S. M. Al-Alawi and S. M. Islam. Principles of electricity demand forecasting. I. Methodologies. *Power Engineering Journal [see also Power Engineer]*, 10(3):139–143, 1996.

[21] J. V. Ringwood, D. Bofelli, and F. T. Murray. Forecasting Electricity Demand on Short, Medium and Long Time Scales Using Neural Networks. *Journal of Intelligent and Robotic Systems*, 31(1):129–147, 2001.

[22] M. G. Lijesen. The real-time price elasticity of electricity. *Energy Economics*, 2006. In press.

[23] NordPool Spot. Market cross points. `http://nordpoolspot.com/reports/systemprice/Marked-Cross-Points/`.

[24] B. Halvorsen and B.M. Larsen. The flexibility of household electricity demand over time. *Resource and Energy Economics*, 23(1):1–18, 2001.

[25] Union for the Co-ordination of Transmission of Electricity. *Statistical yearbook 2005*, 2005.

[26] Norges vassdrags-og energidirektorat (NVE) homepage. Water Reservoir Levels in Norway. `http://nve.no/modules/module_109/publisher_view_product.asp?iEntityId=8820`.

[27] L. O. Fosse, C. J. Giswold, E. Holmqvist, P. T. J. Lund, N. Spjeldnæs, and T. S. Wahl. Kvartalsrapport for kraftmarkedet, 4. kvartal 2005. Technical Report 1, Norges vassdrags- og energidirektorat (NVE), 2006.

[28] European Transmission System Operators (ETSO). *Indicative values for Net Transfer Capacities (NTC) in Europe*, 2006. Available online at: `http://www.etso-net.org`.

[29] S. W. Enevoldsen, P. A. Østergaard, P. E. Morthorst, and R. Moesgaard. Vindkraftens betydning for elprisen i Danmark (eng.: The impact of wind power on power prices in Denmark). Technical report, Aarhus University, Institute of Business and Technology, 2006. Available online at: `http://www.windpower.org/media(1464,1030)/Vind_presser_elprisen.pdf`. Danish only.

[30] Vindmøller i energiplanerne. M1. Pamphlet of facts M1. Published by the Danish Wind Turbine Owners' Association, 2002. Avilable online at `http://www.dkvind.dk`, Danish only.

[31] K. Vogstad. Utilising the complementary charateristics of wind power and hydropower through coordinated hydro production scheduling using the EMPS model. In *Proceedings of Nordic Wind Power Conference*, pages 107–111, March 2000. Avilable online at `http://folk.ntnu.no/klausv/publications/Trondheim2000.pdf`.

[32] H. Holttinen. Optimal electricity market for wind power. *Energy Policy*, 33(16):2052–2063, 2005.

[33] International Energy Agency (IEA). *World Energy Outlook*, 2006.

Appendix A

Source code

A.1 Power market model

```
%%%%%%%%%%%%%%%%%%%%%%%%%%%%%%%%%%%%%%%%
%% power_market_model.m                 %%
%% Thomas Trötscher, 2007               %%
%%%%%%%%%%%%%%%%%%%%%%%%%%%%%%%%%%%%%%%%

%%%%%%%%%%%%%%%%%%%%%%%%%%%%%%%%%%%%%%%%
%%%%%%%%%%%%EDIT BELOW%%%%%%%%%%%%%%%%%%
%%%%%%%%%%%%%%%%%%%%%%%%%%%%%%%%%%%%%%%%
%Each column represents one run.
%All matrixes must have the same number of columns

%LOAD, WIND AND DCHP SERIES.
%Enter 1 through 7 referring to years 2000 - 2007
lwd_series = random_series(1,7,[1 25],'integer');
load_series = repmat(lwd_series,6,1);
wind_series = repmat(lwd_series,3,1);
dchp_series = repmat(lwd_series,2,1);

%HYDRO SERIES
%1 through 21 referring to different inflow series (median = ...
    14)
hydro_series = random_series(1,21,[1 25],'integer');
hydro_series = repmat(hydro_series,2,1);

%WIND PARAMETERS
%The wind power output factor (1=present day installed ...
    capacity)
wind_dkw_multiplier = ones(1,size(load_series,2))*1;
wind_dke_multiplier = ones(1,size(load_series,2))*1;
```

```
28 wind_de_multiplier =  ones(1,size(load_series,2))*1;
29
30 %TRANSFER CONSTRAINTS
31 %Factor to adjust the overall available transfer capacity
32 kappa_multiplier = ones(1,size(load_series,2))*1;
33
34 %THERMAL COST FACTOR
35 %Factor to adjust the overall thermal generation costs
36 tf=1;
37
38 %CONSECUTIVE HYDRO YEARS
39 conhydro = 1; %1=yes
40
41 %%%%%%%%%%%%%%%%%%%%%%%%%%%%%%%%%%%%%%%
42 %%%%%%%%%%%%EDIT ABOVE%%%%%%%%%%%%%%%%%
43 %%%%%%%%%%%%%%%%%%%%%%%%%%%%%%%%%%%%%%%
44
45 if size(load_series,2)≠size(wind_series,2) || size(...
       load_series,2)≠size(dchp_series,2) || ...
46         size(load_series,2)>size(hydro_series,2) || size(...
               load_series,2)>size(wind_dkw_multiplier,2) || ...
47         size(load_series,2)>size(wind_dke_multiplier,2) || ...
               size(load_series,2)>size(wind_de_multiplier,2) || ...
               ...
48         size(load_series,2)>size(kappa_multiplier,2)
49     disp('ERROR: Wrong matrix sizes!');
50     return;
51 end
52
53 % i area
54 % 1 DK-W
55 % 2 DK-E
56 % 3 NO
57 % 4 SE
58 % 5 DE
59 % 6 U
60
61 %DK-W
62 mc{1} = [0 0;           %WIND
63          0 0;           %DCHP
64          170*tf 0.1*tf;       %CENTRAL THERMAL
65          500*tf 3*tf];        %PEAKING THERMAL
66 xmax{1} = [2230 1383.8 2230 135]';
67 xmin{1} = [0    0      0      0]';
68
69 %DK-E
70 mc{2} = [0 0;           %WIND
71          0 0;           %DCHP
72          170*tf 0.081*tf;     %CENTRAL THERMAL
```

```
73          500*tf 3*tf];        %PEAKING THERMAL
74  xmax{2} = [772 819.1 2776.3 135]';
75  xmin{2} = [0   0     0      0]';
76
77  %NO
78  mc{3} = [0 0];          %HYDRO
79  xmax{3} = [23100]';
80  xmin{3} = [0]';
81
82  %SE
83  mc{4} = [0 0;           %HYDRO
84           80 0;          %NUCLEAR
85           160*tf 0.0048*tf;    %THERMAL
86           210*tf 0.4191*tf];   %PEAKING THERMAL
87  xmax{4} = [19167 11632 10435 5584]';
88  xmin{4} = [0     5816  0     0]';
89
90  %DE
91  mc{5} = [0 0;           %WIND
92           80*tf 0;          %NUCLEAR
93           24 0;          %THERMAL REPRESENTING HYDRO
94           130*tf tf*9.639e-4;  %THERMAL
95           170*tf tf*0.0464;    %THERMAL
96           378*tf 0;         %THERMAL
97           378.4*tf tf*0.0052;    %THERMAL
98           440*tf tf*0.1292];   %PEAKING THERMAL
99  xmax{5} = [19000 20700 3185 41500 4500 10000 11750 3250]';
100 xmin{5} = [0     10350 0    0     0    0     0     0]';
101
102 %U
103 mc{6} = [80*tf tf*4.348e-4;   %THERMAL
104          160*tf tf*0.0021;    %THERMAL
105          320*tf tf*0.0096];   %THERMAL
106 xmax{6} = [184000 76000 70000]';
107 xmin{6} = [0      0     0]';
108
109
110 %TRANSFER CONSTRAINTS
111 %Transfer from row to column
112 kappa = [...
113 0       600     1000    630     1350    NaN;
114 600     0       NaN     1810    600     NaN;
115 1000    NaN     0       3620    NaN     700;
116 670     1410    3340    0       600     600;
117 950     600     NaN     600     0       14650;
118 NaN     NaN     700     600     14650   0];
119
120
121 %LOAD TIMESERIES
```

```
load data

%HYDRO PARAMETERS
hydro.no.rmax = data.no.reservoir_capacity; %MWh
hydro.se.rmax = data.se.reservoir_capacity; %MWh
hydro.no.rmedian = interpolate(data.no.median_reservoir_level...
    ,168,8760); % %
hydro.se.rmedian = interpolate(data.se.median_reservoir_level...
    ,168,8760); % %
hydro.no.r = zeros(8761,1); %MWh
hydro.se.r = zeros(8761,1); %MWh
hydro.no.r(1) = hydro.no.rmedian(1)*hydro.no.rmax;
hydro.se.r(1) = hydro.se.rmedian(1)*hydro.se.rmax;

%OVERHAUL SCHEDULE
os = interpolate(data.overhaul,730);

%RUN SIMULATION
tic;
runs = size(load_series,2);
%Allocate output variables, use single precision to save ...
    memory and
%disk-space
price_dkw = zeros(8760,runs,'single');
double_test = zeros(8760,runs);
prod = zeros(8760,runs,24,'single');
transmission = zeros(8760,runs,11,'single');
price_all = zeros(8760,runs,6,'single');
hydro_no = zeros(8761,runs,'single');
hydro_se = zeros(8761,runs,'single');
disp('RUNNING SIMULATION');
for run=1:runs
    %Build load, wind generation, dchp generation and hydro ...
        inflow vectors for this run
    disp(['Run ', num2str(run),' of ', num2str(runs) ,' ...
        commencing']);
    demand = [data.dkw.load{load_series(1,run)} ...
              data.dke.load{load_series(2,run)} ...
              data.no.load{load_series(3,run)} ...
              data.se.load{load_series(4,run)} ...
              data.de.load{load_series(5,run)} ...
              data.u.load{load_series(6,run)}];
    wind = [data.dkw.wind_n{wind_series(1,run)}*2406*...
        wind_dkw_multiplier(run) ...
             data.dke.wind_n{wind_series(2,run)}*737*...
                wind_dke_multiplier(run) ...
             data.de.wind{wind_series(3,run)}*...
                wind_de_multiplier(run)];
    dchp = [data.dkw.dchp{dchp_series(1,run)} ...
```

```
163             data.dke.dchp{dchp_series(2,run)}];
164     %Inflow series are interpolated to yield hourly values. ...
           Multiply by 52/8760 to keep total inflow the same.
165     i = [interpolate(data.no.inflow(:,hydro_series(1,run))...
           ,24*7,8760)*52/8760 ...
166          interpolate(data.se.inflow(:,hydro_series(2,run))...
               ,24*7,8760)*52/8760];
167     if run>1 && conhydro==1
168         hydro.no.r(1) = hydro.no.r(end);
169         hydro.se.r(1) = hydro.se.r(end);
170     end
171     xt = [];
172     transmissiont = [];
173     for t=1:8760
174         %Output progress info
175         if mod(t,219*8)==0
176             disp(['Run ',num2str(run),' ',num2str(100*t/8760)...
                   ,'% completed. Estimated total time left: ', ...
                   num2str(toc*runs*146/(t+(run-1)*8760)-toc/60),...
                   ' of ', num2str(round(toc*runs*146/(t+(run-1)...
                   *8760))),'min']);
177         end
178         %Calculate problem parameters for this timestep
179         loadt = demand(t,:);
180         windt = wind(t,:);
181         dchpt = dchp(t,:);
182         xmax{1}(1) = windt(1);
183         xmax{2}(1) = windt(2);
184         xmax{1}(2) = dchpt(1);
185         xmax{2}(2) = dchpt(2);
186         xmax{5}(1) = windt(3);
187         mc{3}(1,1) = water_value(hydro.no.r(t)/hydro.no.rmax,...
               hydro.no.rmedian(t));
188         mc{4}(1,1) = water_value(hydro.se.r(t)/hydro.se.rmax,...
               hydro.se.rmedian(t));
189         xmax{3}(1) = hydro.no.r(t);
190         xmax{4}(1) = hydro.se.r(t);
191         %Follow overhaul schedule for all thermal power ...
               plants
192         osxmax = xmax;
193         osxmax{1}(2) = xmax{1}(2)*(1-os(t));
194         osxmax{2}(2) = xmax{2}(2)*(1-os(t));
195         osxmax{4}(2) = xmax{4}(2)*(1-os(t));
196         osxmax{4}(3) = xmax{4}(3)*(1-os(t));
197         osxmax{5}(2) = xmax{5}(2)*(1-os(t));
198         osxmax{5}(4) = xmax{5}(4)*(1-os(t));
199         osxmax{5}(5) = xmax{5}(5)*(1-os(t));
200         osxmax{5}(6) = xmax{5}(6)*(1-os(t));
201         osxmax{5}(7) = xmax{5}(7)*(1-os(t));
```

```
202         osxmax{6}(1) = xmax{6}(1)*(1-os(t));
203         osxmax{6}(2) = xmax{6}(2)*(1-os(t));
204         osxmax{6}(3) = xmax{6}(3)*(1-os(t));
205         %Set starting values
206         x0 = [xt; transmissiont];
207         %Solve optimization problem
208         [pt,xt,message,transmissiont] = merit_order(mc,xmin,...
                osxmax,kappa*kappa_multiplier(run),loadt,x0);
209         %Update hydro reservoirs
210         hydro.no.r(t+1) = single_reservoir(xt(9),hydro.no.r(t...
                ),i(t,1),hydro.no.rmax);
211         hydro.se.r(t+1) = single_reservoir(xt(10),hydro.se.r(...
                t),i(t,2),hydro.se.rmax);
212         %Save solution
213         price_dkw(t,run) = pt(1);
214         double_test(t,run) = pt(1);
215         price_all(t,run,:) = pt;
216         prod(t,run,:) = xt;
217         transmission(t,run,:) = transmissiont;
218         hydro_no(t,run) = hydro.no.r(t)/hydro.no.rmax;
219         hydro_se(t,run) = hydro.se.r(t)/hydro.se.rmax;
220     end
221 end
222 %Output info
223 disp('SIMULATION FINISHED');
224 disp(['Elapsed time: ', num2str(round(toc)),'sec.']);
225 filename = ['simulation_result_', datestr(now,30)];
226 save(filename, 'price_dkw', 'price_all', 'prod', '...
       transmission', 'load_series','wind_series','dchp_series','...
       hydro_series','wind_dkw_multiplier','wind_dke_multiplier',...
       'wind_de_multiplier','kappa_multiplier');
227 disp(['Result saved to file: ', filename]);
```

A.2 Generator scheduling

```
1  function [price,prod,message,transmission] = merit_order(mc,...
       mingen,maxgen,icon,demand,x0)
2  %%%%%%%%%%%%%%%%%%%%%%%%%%%%%%%%%%%%%%%%%%%%
3  %% merit_order.m                          %%
4  %% Thomas Trötscher, 2007                 %%
5  %%%%%%%%%%%%%%%%%%%%%%%%%%%%%%%%%%%%%%%%%%%%
6  %[price,prod,message,transmission] = merit_order(mc,mingen,...
       maxgen,icon,demand,x0)
7  %
8  %mc: generator marginal costs in areas
9  %mc_i = a + b*x i.e. cost = a*x + 0.5*b*x^2
10 %Example:
```

```
%Area 1:
% mc{1} = [5 0;
%          50 1;
%          200 5;
%          420 0.1];
%Area 2:
% mc{2} = [1 0;
%          100 2;
%          500 0];
%Area 3:
% mc{3} = [50 3;
%          250 0;
%          150 5];
%maxgen: upper bound on generation
%Example:
%Area 1:
% maxgen{1} = [200;
%              100;
%              500;
%              100];
%Area 2:
% maxgen{2} = [200;
%              250;
%              25];
%Area 3:
% maxgen{3} = [150;
%              250;
%              400];
%mingen: lower bound on generation
%
%icon: transmission capacity
%icon = [0 area1->area2 area1->area3;
%        area2->area1 0 area2->area3;
%        area3->area1 area3->area2 0]
%Normally symmetric about the main diagonal
%Enter NaN if there is no transmission line
%Example:
% icon = [0 100 50;
%         100 0 NaN;
%         50 NaN 0];
%demand: Demand in area [1 2 3 ... n]
%Example:
% demand = [1000 250 500]';
DEBUGGING = 0;
%%%%%%%%%%%%%%%%%%%%%%%%%%%%%%%%%%
%Reformulate problem on standard
%form and solve
%%%%%%%%%%%%%%%%%%%%%%%%%%%%%%%%%%

```

```
%number of areas
numarea = length(mc);
%number of possible interconnectors
numcon = (numarea^2-numarea)/2;
ab = cat(1,mc{:},zeros(numcon,2));
%number of generators
numgen = size(ab,1)-numcon;
%Form equality constraint matrices
Aeq1 = [];
for i = 1:numarea
    Aeq1 = blkdiag(Aeq1,ones(1,size(mc{i},1)));
end
Aeq2 = zeros(numarea,numcon);
j = 1;
k = 1;
for i = 1:numcon
    if j < numarea
        j = j + 1;
    else
        k = k + 1;
        j = 1 + k;
    end
    Aeq2(k,i) = -1;
    Aeq2(j,i) = 1;
end
Aeq = cat(2,Aeq1,Aeq2);
beq = demand;
%No inequality constraints
A= [];
b = [];
%Bounds
Z1 = triu(icon,1)';
Z2 = tril(icon,-1);
z1=Z1(Z1~=0);
z2=Z2(Z2~=0);
%z1(isnan(z1))=0;
%z2(isnan(z2))=0;
%Lower bounds
lb1 = cat(1,mingen{:}); %Generators
lb2 = -z2; %Transmission lines
lb = cat(1,lb1,lb2);
%Upper bounds
ub1 = cat(1,maxgen{:}); %Generators
ub2 = z1; %Transmission lines
ub = cat(1,ub1,ub2);
%Remove unnecessary variables
nnan = ~(isnan(lb) & isnan(ub));
Aeq = Aeq(:,nnan);
lb = lb(nnan);
```

```
109 ub = ub(nnan);
110 %Form object function matrices
111 f = ab(nnan,1);
112 H = diag(ab(nnan,2));
113 %Output error message if generation is insufficient to cover ...
       demand
114 if sum(ub1)<sum(demand)
115     disp('Not sufficient generation capacity. Exiting!');
116     beep; pause(.1); beep; pause(.1); beep;
117     return;
118 end
119 %Generate starting values
120 if isempty(x0)
121     gen0=[];
122     for i=1:numarea
123         gen0=cat(1,gen0,initx(mingen{i},maxgen{i},demand(i)))...
              ;
124     end
125     x0 = cat(1,gen0,zeros(size(ub2)));
126     x0 = x0(nnan);
127 end
128 %Set optimization options
129 options = optimset('Display','off','LargeScale','off');
130 %Try to solve with quadprog, faster, but sometimes fails.
131 [x,fval,exitflag,output,lambda] = quadprog(H,f,A,b,Aeq,beq,lb...
       ,ub,x0,options);
132 if exitflag ~= 1
133     %try another solver
134     %disp('Quadprog failed. Trying fmincon');
135     options = optimset('Display','off','LargeScale','off','...
          TolFun',0.1,'TolX',1e-3,'TolCon',1e-3,'MaxFunEvals',1...
          e6);
136     %options = optimset('Display','off','LargeScale','off','...
          MaxFunEvals',1e6);
137     [x,fval,exitflag,output,lambda] = fmincon(@(x)0.5*x'*H*x+...
          f'*x,x0,A,b,Aeq,beq,lb,ub,[],options);
138     if exitflag<1
139         disp('ERROR! Could not solve problem!')
140         output.message
141         [lb x ub]
142         lambda.eqlin
143         beep; pause(.1); beep; pause(.1); beep;
144         return
145     end
146 end
147 if DEBUGGING == 1
148     if x > ub || x < lb
149         disp('Bounds exceeded');
150     end
```

```
151     transmission = sum(icon,2);
152     if (transmission(1)+demand(1)) < (-1e-2 + maxgen{1}(1) + ...
            maxgen{1}(2))
153         disp(['Overflow! Price = ', num2str(-lambda.eqlin(1))...
                ])
154         if -lambda.eqlin(1)>1e-2
155             disp('Price not zero!!!!');
156             [lb x ub]
157             pause
158         end
159     end
160     if (x(1)+x(2))<(-1e-2 + maxgen{1}(1) + maxgen{1}(2))
161         disp('Capacity not utilized');
162         if -lambda.eqlin(1)>1e-2
163             disp('Price not zero');
164         end
165         disp(['Price = ', num2str(-lambda.eqlin(1))])
166     end
167 end
168 price = -lambda.eqlin;
169 prod = x(1:numgen);
170 transmission = x(numgen+1:end);
171 message = output.message;
```

A.3 Initial solution

```
1  function x0 = initx(xmin,xmax,demand)
2  %%%%%%%%%%%%%%%%%%%%%%%%%%%%%%%%%%%%%%%%
3  %% initx.m                              %%
4  %% Thomas Trötscher, 2007               %%
5  %%%%%%%%%%%%%%%%%%%%%%%%%%%%%%%%%%%%%%%%
6  %Calculate an initial solution for the merit order function,
7  %works best when generators are sorted from low to high cost
8  x0 = xmin;
9  for g = 1:length(x0)
10     r = xmax-x0;
11     tot = sum(x0);
12     if tot≥ demand
13         return;
14     elseif r(g)<(demand-tot)
15         x0(g) = xmax(g);
16     else
17         x0(g) = x0(g)+demand-tot;
18         return;
19     end
20 end
```

A.4 Water value

```
function wv = water_value(r,rmean)
%%%%%%%%%%%%%%%%%%%%%%%%%%%%%%%%%%%%%%%%%%%%
%% water_value.m                          %%
%% Thomas Trötscher, 2007                 %%
%%%%%%%%%%%%%%%%%%%%%%%%%%%%%%%%%%%%%%%%%%%%
%function wv = water_value(r,rmean)
% Used to determine the water value as a function of the ...
    reservoir level
% and historical mean reservoir level
% r           : current reservoir level
% rmean       : reference (median) reservoir level

%Convert 0.xx to xx%
r=r*100;
rmean=rmean*100;

if r > 99.99
    %Water value is zero when the reservoir is full
    wv = 0;
    return
end

deviation = r - rmean;

wv = -1.0136*sign(deviation)*(abs(deviation))^1 -0.0138*sign(...
    deviation)*(abs(deviation))^3 + 200;
```

A.5 Single reservoir model

```
function r = single_reservoir(x, r_last, i, rmax)
%%%%%%%%%%%%%%%%%%%%%%%%%%%%%%%%%%%%%%%%%%%%
%% single_reservoir.m                     %%
%% Thomas Trötscher, 2007                 %%
%%%%%%%%%%%%%%%%%%%%%%%%%%%%%%%%%%%%%%%%%%%%
%function r = single_reservoir(x, r_last, i, h)
%   r_last : reservoir level at the beginning of the previos ...
    timestep
%   x      : generation during the last timestep
%   i      : inflow during the last timestep
%   rmax   : reservoir maximum
%   r      : reservoir level at the beginnning of this ...
    timestep

```

```
%Calculate spill
s = max(r_last+i-x-rmax,0);
%Calculate new reservoir level
r = r_last + i - x - s;
%Error checking
if r>rmax | r<0
    disp('ERROR: Reservoir level out of bounds!')
end
```

A.6 Random series

```
function r = random_series(minvalue,maxvalue,ssize,integer)
%%%%%%%%%%%%%%%%%%%%%%%%%%%%%%%%%%%%%%%%%%%%%%%
%% random_series.m                              %%
%% Thomas Trötscher, 2007                       %%
%%%%%%%%%%%%%%%%%%%%%%%%%%%%%%%%%%%%%%%%%%%%%%%
%function r = random_series(minvalue,maxvalue,ssize,integer)
%Used to generate a matrix of random integers between ...
    minvalue and maxvalue
rand('state',sum(100*clock));
if nargin == 4
    if integer=='integer'
        r = ceil(rand(ssize)*(maxvalue-minvalue+1)) + ...
            minvalue - 1;
    end
else
    r = rand(ssize)*(maxvalue-minvalue) + minvalue;
end
```

A.7 Load profile

```
function load = load_profile(lpmatrix, wb, wbpeak, stddev, ...
    startday)
%%%%%%%%%%%%%%%%%%%%%%%%%%%%%%%%%%%%%%%%%%%%%%%
%% load_profile.m                               %%
%% Thomas Trötscher, 2007                       %%
%%%%%%%%%%%%%%%%%%%%%%%%%%%%%%%%%%%%%%%%%%%%%%%
% Function to create hourly load data for a year (8760 hours)...
     based on a
% load profile matrix for the 3. Wednesday every month.
%
% function load = load_profile(lpmatrix, wb, stddev, startday...
    )
%   lpmatrix    :   12x24 Matrix (months x hours) of load ...
    data from UCTE
```

```
11 %   wb          :   Weekend bias. Relative reduction in load ...
       on weekends
12 %   wbpeak      :   Weekend peak bias. Relative peak ...
       reduction on weekends
13 %
14 %   OPTIONAL
15 %   stddev      :   Daily std. dev. in load to introduce ...
       randomness.
16 %                   Default 0
17 %   startday    :   Starting weekday (1=monday 7=sunday) ...
       Default: 1
18 if nargin == 3
19     stddev = 0;
20     startday = 1;
21 elseif nargin == 4
22     startday = 1;
23 end
24 randomness = interp(randn(1,365)*stddev*mean(mean(lpmatrix))...
       ,24);
25 %Calculate the weekend load profile matrix
26 weekendlpm = (lpmatrix - min(lpmatrix')'*ones(1,24))*wb*...
       wbpeak + min(lpmatrix')'*ones(1,24)*wb;
27 for t = 1:8760
28     if (dayofweek(t,startday) == 6) | (dayofweek(t,startday) ...
           == 7)
29         %Use the weekend load profile
30         lpm = weekendlpm;
31     elseif (dayofweek(t,startday) == 1) & (timeofday(t)<7)
32         %Use the weekend load profile
33         lpm = weekendlpm;
34     elseif (dayofweek(t,startday) == 5) & (timeofday(t)>18)
35         %Use the weekend load profile
36         lpm = weekendlpm;
37     else
38         %Use the weekday load profile
39         lpm = lpmatrix;
40     end
41     if timeofmonth(t)<730*(3/4)
42         %before 3rd wednesday of month
43         if monthofyear(t)>1
44             baseload = lpm(monthofyear(t)-1,timeofday(t))...
                   *(730*(3/4)- timeofmonth(t))/730 + lpm(...
                   monthofyear(t),timeofday(t)) * (timeofmonth(t)...
                   +730*(1/4))/730;
45         else
46             baseload = lpm(12,timeofday(t))*(730*(3/4)-...
                   timeofmonth(t))/730 + lpm(1,timeofday(t)) * (...
                   timeofmonth(t)+730*(1/4))/730;
47         end
```

```
48      else
49          %after 3rd wednesday of month
50          if monthofyear(t)<12
51              baseload = lpm(monthofyear(t),timeofday(t))...
                    *(730*(7/4)-timeofmonth(t))/730+lpm(...
                    monthofyear(t)+1,timeofday(t)) * (timeofmonth(...
                    t)-730*(3/4))/730;
52          else
53              baseload = lpm(12,timeofday(t))*(730*(7/4)-...
                    timeofmonth(t))/730+lpm(1,timeofday(t)) * (...
                    timeofmonth(t)-730*(3/4))/730;
54          end
55      end
56      %Add randomness
57      load(t) = baseload + randomness(t);
58  end
59
60  %--------------------
61  %SUBFUNCTIONS
62  function h = timeofday(hours)
63  h = mod(hours-1,24)+1;
64  return
65
66  function m = timeofmonth(hours)
67  m = mod(hours-1,730)+1;
68  return
69
70  function day = dayofyear(hours)
71  day = floor(365*(hours-1)/8760)+1;
72  return
73
74  function month = monthofyear(hours)
75  month = floor(12*(hours-1)/8760)+1;
76  return
77
78  function dow = dayofweek(hours,startday)
79  dow = mod(dayofyear(hours)-1,7)+startday;
80  if dow>7
81      dow = dow-7;
82  end
83  return;
```

Appendix B

Wind speed and temperature correlation

Figure B.1 shows scatter plots of wind speed versus temperature at 10 different stations located along the coast of Norway. Monthly mean wind speed and monthly mean temperature for the years 1966 to 2006 has been used. The data has been split according to season and fitted to a linear regression model.

The figure shows that there is a positive relationship between temperature and wind speed during the winter months, a negative relationship during the summer months and no conclusive result for spring and fall.

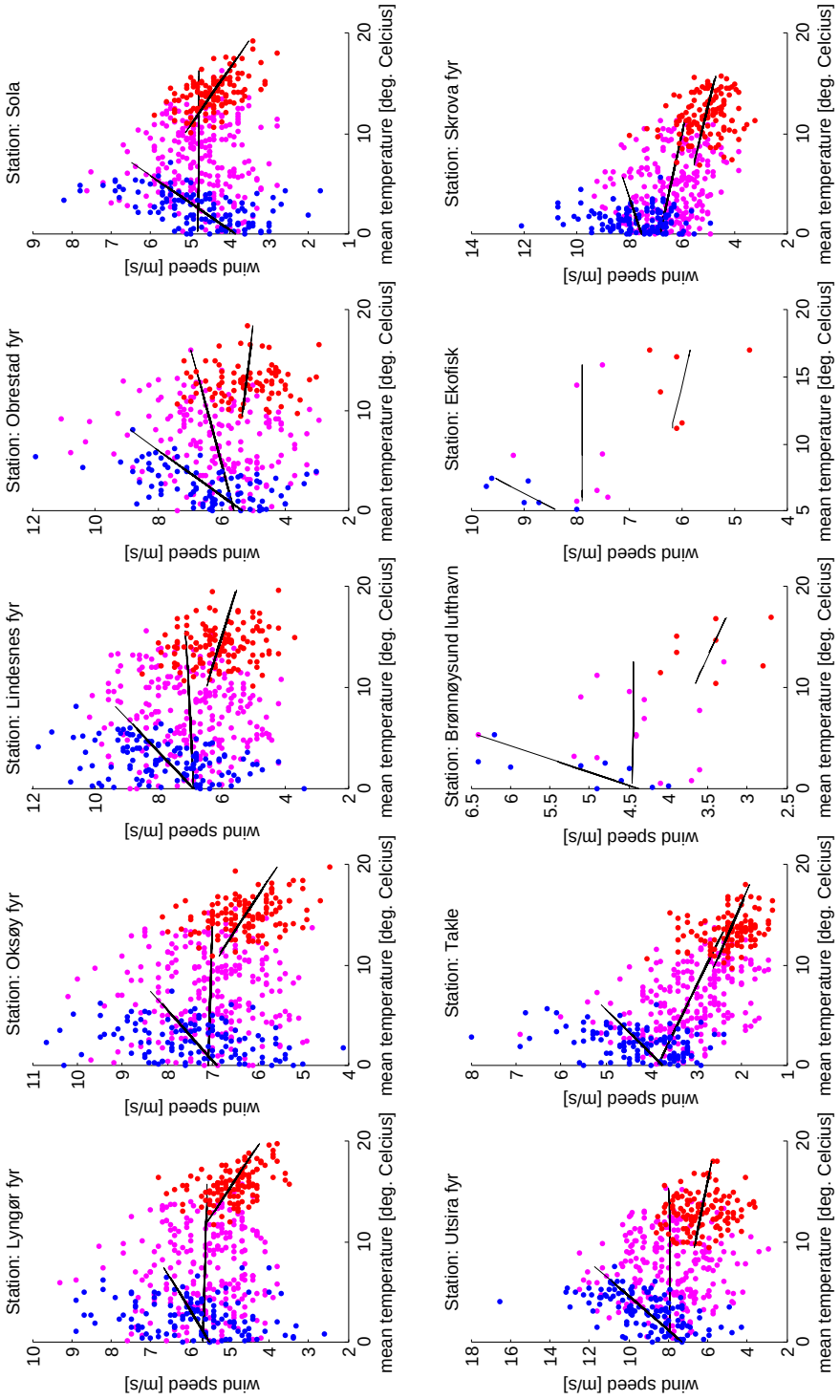

Figure B.1: Wind speed vs. temperature separated on season (blue=winter, red=summer, magenta=spring and fall).